Mitigation of cascading failures by real-time controlled islanding and graceful load shedding

Stephan Koch, Spyros Chatzivasileiadis, Maria Vrakopoulou and Göran Andersson
EEH - Power Systems Laboratory, ETH Zurich, Physikstrasse 3, 8092 Zurich, Switzerland
E-mail: {koch,spyros,vrakopoulou,andersson}@eeh.ee.ethz.ch

Abstract

This paper presents an emergency control strategy, which serves to counteract a cascading disturbance in a large power system that would eventually lead to a blackout. The strategy is composed of two parts: after a disturbance, a real-time controlled islanding algorithm based on slow coherency of synchronous generators and k-means clustering splits the system into autonomously operating parts. The imbalances between load and generation are then accounted for by generator tripping in the generation-rich islands and a novel type of under-frequency load shedding in the load-rich islands, if the available primary control reserves are insufficient or too slow to stabilize the frequency. As opposed to the under-frequency relays in substations which are often used nowadays, the system considered here utilizes a "smart home" communication and control infrastructure for assigning frequency thresholds to individual appliances owned by consumers. Pervasive availability of this infrastructure is assumed. The strategy is evaluated in time-domain simulations using the IEEE 118-bus system.

I. Introduction

Traditionally, transmission grids used to serve as a means to transport electricity from the power plants to the consumers, and as a tool for mutual assistance in case of emergencies. In the recent years, however, they have become a complex platform for shifting growing power volumes across entire continents. Market developments result in higher cross-border and long-distance energy exchanges. Other cross-continental power flows result from the fast and successful development of intermittent energy generation with limited predictability, e.g. wind power. These developments were not taken into account in the original system design, and consequently lead to a system operation which is closer to the stability limits.

In a highly loaded power system in which the operational safety margins tend to be reduced more and more, it is more likely for a common disturbance to drive the system into a wide-area blackout through cascading events. This indicates the need of a more coordinated solution to mitigate the potential impact of failures. This paper proposes a new methodology to alleviate the undesirable effects that large disturbances might lead to. The proposed scheme consists of a rapid controlled islanding method followed by a novel customer-level load shedding policy. Both techniques can also be used separately, although significant synergies can arise from a joint implementation.

Controlled islanding partitions the disturbed system into smaller islands based on slow-coherent generators and considering the minimum load-generation imbalance applying machine learning techniques. This action prevents the spreading of the failure in the whole system and therefore leads to a smaller restoration time. The customer-level load shedding serves to mitigate the impact of the power imbalance inside each island. This decentralized shedding capability is enabled by the usage of "smart home" infrastructure which interconnects individual household appliances, allowing to disconnect low-priority load for disturbance mitigation in order to keep the impact on customer comfort low. Benefits of this scheme are particularly evident when large amounts of generation are present on the distribution level, as conventional load shedding would lead to an additional loss of generation.

The proposed islanding and customer-level load shedding approach is tested on the IEEE 118-bus, 19-generator benchmark network. Its effectiveness is verified in the presence of a disturbance which is likely to cause a cascading failure if left unmitigated.

This article is organized as follows: Section II presents the controlled islanding method, describing the k-means clustering methodology for the partitioning of the power system network. Section III introduces the customer-level load shedding system, which includes some literature review, elaboration of the system design, mathematical formulation of the load shedding problem and a tuning method for the frequency thresholds[1]. Section IV presents a case study including dynamic simulations of the 118-bus system, in which both the controlled islanding and the under-frequency load shedding are simulated to mitigate the impact of a line fault moving the system towards angle instability. Conclusions and suggestions for further research are presented in section V.

II. Controlled Islanding

A. Literature Review

Controlled islanding has been proposed by a handful of researchers as an appropriate corrective control measure against large disturbances. Partitioning the system into subnetworks with slightly reduced capacity helps to contain the disturbance and leads to a faster restoration of the network to its initial state. If the controlled islanding strategy is successful, then less or – optimally – none of the generators will trip and as a result less load shedding will be required.

Several approaches can be found in the literature about how to

[1]Note that the nomenclatures for describing the controlled islanding and the load shedding parts are distinct, i.e. the same symbols may be used for different purposes. As both parts can be formulated and used separately, merging the notation does not seem necessary.

978-1-4244-7467-7/10/$26.00

develop a proper strategy for controlled islanding. A controlled islanding approach based on graph spectral methods is described in [1]. In [2] an off-line method is proposed based on a slow coherency grouping of the generators and a determination of the minimum cut-sets. The identification of the slow-coherent generators is based on the method described in [3] with a modification called "tolerance-based slow coherency" in order to deal with large systems and to achieve more precise results. The objective is to find states with the same content of disturbed modes. Although the slow coherency method is based on a linearized model, results have indicated that it accurately captures the dynamic behavior of the nonlinear system [2].

Several researchers proposed different methods for a real-time determination of the optimal island boundaries during the last years. An extensive study of the 118-bus system with a graph-theoretic approach called OBDD (ordered binary decision diagram) and transient simulations is presented in [4]. Methods based on graph theory are also presented in [5], [6]. Hybrid methods have also appeared in the literature, where first the dynamic characteristics of the network are identified off-line, and in real time the algorithm tries to find the optimal partitions. In [7] the author identifies the coherent generators with the Krylov Subspace Method [8] off-line and then suggests a method for determining the islands with the least load-generation imbalance in real time.

Different criteria are employed in order to find the optimal island partitioning. The most commonly used is the minimum load-generation imbalance criterion, as all methods attempt to determine islands where minimum load shedding should occur. Certain approaches incorporate also the rotor angle of the generators. In [4] and [6] the loss of synchronism of the generators is taken into account, while in [4], additionally, the capacity limits of the transmission lines are considered.

In the approach presented in this paper, a hybrid method is adopted. A slow coherency grouping algorithm is implemented, as described in [3], in order to provide an indication of the dynamic behavior of the generators during a disturbance. Subsequently, a method based on k-means clustering is introduced in order to identify in real time the points where the network must be split after a large disturbance. The criteria for the boundaries are the rotor angle deviation among the generators and the minimum load-generation imbalance. The presented algorithm acts fast and is modular, allowing for the incorporation of different criteria for the identification of the islands. It is able to adapt to the current situation of power generation and consumption, which can prove advantageous in a system with a high penetration of intermittent renewable energy generation units.

In the following paragraphs of this section, first the k-means clustering algorithm is presented and then the adaptations for the use in controlled islanding are described. Finally, the method for the integration of the different criteria is introduced.

B. Theoretical Background – k-means

The k-means algorithm was originally designed for observations in the Euclidean space aiming to partition N observations into K clusters, in which each observation belongs to the cluster with the nearest mean. A cluster is defined as a group of data points whose inter-point distances are small compared with the distances to points outside of the cluster. Introducing a set of vectors μ_k, where $k = 1, \ldots, K$, we can associate each μ_k with the k^{th} cluster. We can think of μ_k as representing the centers of the clusters. The goal is to find an assignment of data points to clusters, as well as a set of vectors $\{\mu_k\}$, such that the sum of the squares of the distances of each data point to its closest vector μ_k is minimum [9].

Defining some notation, we introduce for each data point $\mathbf{x}_n$ a corresponding set of binary indicator variables $r_{nk} \in \{0, 1\}$, where $k = 1, \ldots, K$. Variable r_{nk} describes which of the K clusters the data point $\mathbf{x}_n$ is assigned to, so that if data point $\mathbf{x}_n$ is assigned to cluster k then $r_{nk} = 1$, and $r_{nj} = 0$, for $j \neq k$. The objective function can now be defined as:

$$J = \sum_{n=1}^{N} \sum_{k=1}^{K} r_{nk} \|\mathbf{x}_n - \mu_k\|^2 \quad . \tag{1}$$

The goal is to find values for the $\{r_{nk}\}$ and the $\{\mu_k\}$ so as to minimize J. This is achieved through an iterative procedure. First, some initial values for the $\{\mu_k\}$ are selected. Then, in the first phase J is minimized with respect to the r_{nk}, keeping the μ_k fixed. In the second phase J is minimized with respect to the μ_k, keeping the r_{nk} fixed. In mathematical terms the procedure can be summarized as follows:

1st Phase:

$$r_{nk} = \begin{cases} 1 & \text{if } k = \text{argmin}_j \|\mathbf{x}_n - \mu_j\|^2 \\ 0 & \text{otherwise} \end{cases} \quad , \tag{2}$$

2nd Phase:

$$\min_{\mu_k} J \Rightarrow \left.\frac{dJ}{dt}\right|_{\mu_k} = 0 \Rightarrow$$

$$2 \sum_{n=1}^{N} r_{nk} (\mathbf{x}_n - \mu_k) = 0 \Rightarrow$$

$$\mu_k = \frac{\sum_n r_{nk} \mathbf{x}_n}{\sum_n r_{nk}} \quad . \tag{3}$$

This two-stage optimization is repeated until convergence. As each phase reduces the value of the objective function J, convergence of the algorithm is assured.

C. k-means for Controlled Islanding

According to the approach proposed in this paper, the controlled islanding can be viewed as a clustering problem, where the power system buses are partitioned into k clusters. Some adaptations of the algorithm described above are needed in order to be applied to the controlled islanding problem. As observations we consider the buses, which must be clustered according to a *minimum distance* objective function.

We model the power system as a weighted, undirected graph $G = (V, E)$, where $V = \{v_1, \ldots, v_n\}$ is the set of vertices

representing the n power system nodes, $E = \{e_{ij}\}$ is the set of edges corresponding to the m power lines and $W = \{w_{ij}\}$ is the set of weights assigned to the edges, i.e. W: $E \rightarrow \mathbf{R}$. From E and W we can build a Weighted Adjacency Matrix of the graph, $A = [a_{ij}]$, where

$$a_{ij} = \begin{cases} 1 \cdot w_{ij} & \text{if } e_{ij} \in E \quad , \\ 0 & \text{otherwise} \quad . \end{cases}$$

With the weights representing the distances between the nodes, we can influence how close or how far the nodes are from each other. The following criteria are used in this paper in order to determine the weights:

1) The groups of coherent generators according to the ρ slowest modes,
2) The rotor angle difference among the generators,
3) The load-generation active power imbalance of the islands.

A more detailed description of how the weights are determined will follow in the next sections. In the rest of this section the k-means based algorithm for the partitioning of the system will be described.

From the Weighted Adjacency Matrix the shortest path between any two buses can be calculated. The weight of path $p = \{v_0, v_1, ..., v_k\}$ is the sum of the weights of its constituent edges [10]:

$$w(p) = \sum_{i=1}^{k} w(v_{i-1}, v_i) \quad . \tag{4}$$

The shortest path weight from u to v is defined by:

$$\delta(u, v) = \begin{cases} \min(w(p) : u \rightsquigarrow v) & \text{if exists a path from } u \text{ to } v, \\ \infty & \text{otherwise} \ . \end{cases} \tag{5}$$

The calculated shortest path weights, which we will refer to as distances, are stored in the Distances Matrix $D = [d_{ij}]$, where $d_{ij} = \delta(bus_i, bus_j)$. No distance value will be infinite as there are no isolated buses or islands (before the controlled islanding) in the power system under study.

The Distances Matrix is received as an input for the k-means algorithm. In the first step, a set of buses $\{\mu_1, \ldots, \mu_k\}$, where k is the number of clusters, is selected. The $\{\mu_k\}$ correspond to the center of the clusters of the k-means algorithm. For the sake of simplicity, we will refer to them as centroids. The rest of the buses are assigned to one of the clusters according to the function:

$$r_{nk} = \begin{cases} 1 & \text{if } k = \text{argmin}_j w_{nj} \quad , \\ 0 & \text{otherwise} \quad . \end{cases} \tag{6}$$

In the second phase, in each cluster the bus with the minimum distance from all the rest of the buses is selected as the new centroid for this cluster. In mathematical formulation this can be written as

$$\mu_k = \text{argmin}_j \sum_{i=1}^{M} w_{ij} \quad , \tag{7}$$

where w_{ij} is the distance between buses bus_i and bus_j, with $bus_i, bus_j \in C_k$ (C_k being the cluster), and M being the total number of buses belonging to this cluster. As soon as the new centroids have been determined, the algorithm returns to the first step, where it assigns again all the buses to clusters. The algorithm converges when the set of centroids remains the same for two consecutive steps.

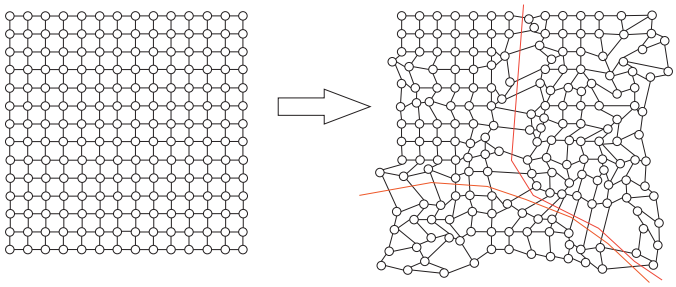

Fig. 1. Illustration of the modification of the Weighted Adjacency Matrix and the k-means controlled islanding

As will be described in the next sections, the k-means approach exhibits certain advantages. It is fast (solution obtained in some tens to some hundreds of milliseconds), modular (different criteria can be incorporated) and adaptive to the currently existing conditions. Therefore, it can act in real time.

Giving a general overview of the proposed approach, the controlled islanding algorithm is divided into two parts. One is executed off-line and the other runs at real time right after a disturbance occurs. For the off-line part, the weights are initialized to $w_{ij} = 1, \forall i, j$, and subsequently get modified according to the slow coherency grouping. In this way, the distances between the generating nodes which belong to the same coherent group are decreased. This modified matrix is taken as an input for the second part of the algorithm. In the second part, the matrix is further modified so that the rotor-angle differences between the generators and the load-generation imbalance are taken into account. For example, the distances w_{ij} between load nodes and nearby generators get further decreased. As nodes leading to a smaller load-generation imbalance "move" closer together, there is greater probability that the k-means algorithm groups these nodes together. Fig. 1 gives an illustrative representation of the approach, while Fig. 2 presents the different steps of the algorithm in a flow chart.

D. Slow Coherency

The identification of the coherent groups is based on the method described in [3]. More specifically, an eigenvalue analysis is performed and the ρ slowest modes of the system are identified. The generators are being grouped according to these slowest modes. Synoptically, the steps for the slow coherency grouping are the following:

1) Assuming the loads as constant impedances, we perform a Ward Reduction of the system, keeping only the generator buses. The method followed in this step is the node elimination by Kron Reduction. The k^{th} row and k^{th} column can be eliminated from a matrix $P = [p_{ij}]$ with the following elementary operation:

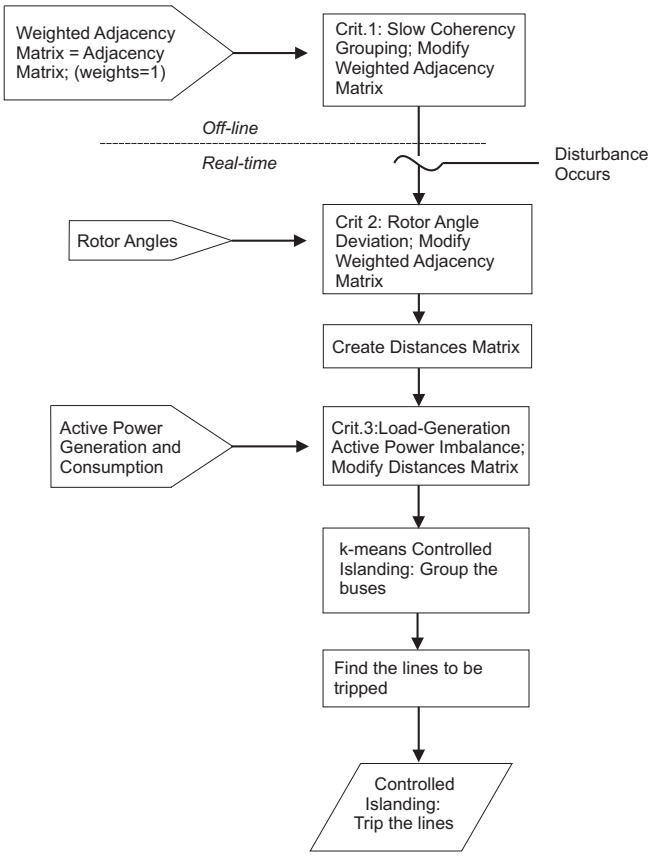

Fig. 2. Flow chart of the k-means controlled islanding algorithm

$$p_{kj}^{\text{new}} = p_{kj} - \frac{p_{kn}p_{nj}}{p_{nn}}. \tag{8}$$

In our case the matrix P is the Admittance Matrix of the system, from which all the rows and columns not corresponding to generator buses will be eliminated, so that $P^{\text{new}} = Ybus^{\text{reduced}}$.

2) Calculate the matrix K. K is a matrix of entries k_{ij}, with:

$$k_{ij} = v_i v_j B_{ij} cos(\delta_i - \delta_j), \tag{9}$$

$$k_{ii} = -\sum_{j=1, j\neq i}^{n} k_{ij}, \tag{10}$$

where v_i, v_j are the node voltages, B_{ij} is the imaginary entry i, j of the reduced admittance matrix $Ybus^{\text{reduced}}$ and δ_i, δ_j are the voltage angles.

3) Calculate the $M^{-1}K$ matrix where $M = diag(m_1, m_2, \ldots, m_n)$, $m_i = \frac{2H_i}{\Omega}$, H is the inertia, Ω is the base angular frequency.
4) Calculate the eigenvalues and eigenvectors of the $M^{-1}K$ matrix.
5) Select the ρ slowest modes, i.e. the ρ eigenvalues with the smallest absolute value, and identify the eigenvectors belonging to these eigenvalues. Form an eigenbasis matrix V from these eigenvectors.
6) Apply Gaussian elimination with complete pivoting to matrix V in order to obtain the set of reference states. Rearrange the rows of the initial V matrix, so that $V = [V_1 V_2]^T$ with V_1 referring to the reference states.
7) Compute L for the set of reference states chosen in the previous step, with $L = [\ell_{ij}]$ and $L = V_2 V_1^{-1}$.
8) Construct the matrix L_g which defines the states in each area. L_g is called the grouping matrix with $L_g = [g_{ij}]$, where $g_{ij} \in \{0, 1\}$. The value closer to 1 in each row of the L matrix is set to 1 and all the rest are set to zero.

The algorithm groups the generators into ρ coherent groups with respect to the ρ slowest modes. The parameter ρ must be given as an input. In matrix L_g the machines are strictly assigned to only one of these groups. For a more detailed description of the algorithm, the reader can refer to [3].

1) Modification of the Weighted Adjacency Matrix: The slow coherency groups give us a first indication of how the generators might behave when a disturbance occurs. Generators belonging to the same group have the tendency to swing together. As soon as the groups of the generators have been determined, the Weighted Adjacency Matrix is modified. The distances between generators belonging to the same coherent group are decreased. The following procedure is followed:

- For every pair of generators belonging to the same coherent group do:
  1) Find the shortest path connecting two generator buses g_i, g_j. Let $path(g_i, g_j) = \{bus_1, bus_2, \ldots, bus_i, \ldots, bus_{n-1}, bus_n\}$, with $bus_1 = g_i$ and $bus_n = g_j$.
  2) Decrease the distances between the buses:

$$\begin{aligned} w(bus_1, bus_2) &= C_{\text{coh}} w(bus_1, bus_2) \\ &\vdots \\ w(bus_i, bus_j) &= C_{\text{coh}} w(bus_i, bus_{i+1}) \\ &\vdots \\ w(bus_{n-1}, bus_n) &= C_{\text{coh}} w(bus_{n-1}, bus_n) \end{aligned} \quad , \quad \text{where } C_{\text{coh}} < 1.$$

E. Criterion 2: Angle Deviation

The Modification of the Weighted Adjacency Matrix based on the relative angle deviation takes place in real time. The objective of this step is to decrease the distances between generators with similar rotor angles and at the same time increase the distances between groups of generators with deviating rotor angles. The algorithm receives as an input the groups of machines with similar angles, which are being identified when the disturbance is detected. Its output is the modified Weighted Adjacency Matrix. The procedure is the following:

- For every pair of generators belonging to different groups do:
  1) Find all the paths connecting two generator buses g_i, g_j which belong to different groups[2]. Let $path(g_i, g_j) =$

[2]Finding all the paths connecting two vertices of a graph is an NP problem. But given the fact that we are interested only in the branches emanating from g_i and the branches arriving at g_j (see next step of the algorithm), the search, with certain constraints, can have polynomial complexity.

$\{bus_1, bus_2, \ldots, bus_i, \ldots, bus_{n-1}, bus_n\}$, with $bus_1 = g_i$ and $bus_n = g_j$.

2) For every path, increase the following distances: $w(bus_1, bus_2) = w(bus_{n-1}, bus_n) = C_{\text{diffang}}$, where $C_{\text{diffang}} >> 1$.

- For every pair of generators belonging to the same group do:
  1) Find the shortest path connecting two generator buses g_i, g_j.
  2) Decrease the distances between the buses:

$$\begin{aligned} w(bus_1, bus_2) &= C_{\text{simang}} w(bus_1, bus_2) \\ &\vdots \\ w(bus_i, bus_j) &= C_{\text{simang}} w(bus_i, bus_j) \\ &\vdots \\ w(bus_{n-1}, bus_n) &= C_{\text{simang}} w(bus_{n-1}, bus_n) \end{aligned} \quad , \quad \text{where } C_{\text{simang}} < 1.$$

Splitting the system into islands with similar relative angles plays an important role for the stability of the islands. Therefore, the modification of the weights in this step is quite brute. Right after this step the Distances Matrix is formed.

F. Criterion 3: Load-Generation Active Power Imbalance

This part of the algorithm also takes place in real time. As an input the Distances Matrix is required, as well as the current active power production and consumption on all the buses. The algorithm determines which neighboring load buses each generator can supply with power. The distances between these buses and the generator decrease, while for the rest the distances remain unchanged. The distances between neighboring generator buses are not decreased either. For each generating bus the procedure is as follows:

1) Identify the rest of the generating buses and set their distance to $\text{dist}(genbus, i) = \max_j \text{dist}(genbus, j) + 1$.
2) Sort the buses from minimum to maximum distance from the selected generating bus.
3) Form a column vector lp with the consumed active power corresponding to the sorting of the load buses in the previous step.
4) Calculate the cumulative sum of the lp, i.e. in each row is stored the sum of the active power of the previous rows; store it in the vector $sumlp$.
5) Subtract from each row of the vector $sumlp$ the active generating power of the selected initial generating bus and store it in the vector $netsumlp$.
6) The rows of the $netsumlp$ vector with negative elements correspond to the buses which can be supplied from the selected generating bus. These buses should decrease by a certain reduction factor their distance from the selected generating bus. The reduction factor is defined as $C_{\text{imbalance}}$, with $C_{\text{imbalance}} < 1$.

As soon as the Distances Matrix is modified, the k-means clustering is ready to take action.

G. k-means Clustering Parameters

Controlled islanding based on the k-means approach presents certain advantages. The time needed for the execution of the real-time part of the algorithm is in the scale of milliseconds (see Table I). Therefore, it can act in real time and adapt to the current situation, potentially taking into account intermittent power generation, when calculating the load-generation imbalance. It is also modular as different criteria can be incorporated by modifying appropriately the Weighted Adjacency Matrix or the Distances Matrix. The successful determination of the islands depends on certain parameters. In order for the algorithm to behave optimally in most cases, it is important to set appropriately the factors $C_{\text{coh}}, C_{\text{diffangle}}, C_{\text{simangle}}, C_{\text{imbalance}}$ for the different criteria, the number of clusters, as well as the initial set of centroids.

In the presented algorithm, the number of clusters is defined to be the same as the number of groups determined in the angle deviation part. The buses which will serve as the initial set of centroids are defined as the generating buses with the largest power production in each of the groups determined in the angle deviation part. The following values are set for the rest of the parameters: $C_{\text{coh}} = 0.8, C_{\text{diffangle}} = 100, C_{\text{simangle}} = 0.1, C_{\text{imbalance}} = 0.7$. Execution times have been measured for all the parts of the controlled islanding algorithm. The power system used was the IEEE 118-bus system with 19 generators [11], which is split in 2 groups. The mentioned time period is the average time needed for the execution of each algorithm part after completing 20 iterations. The average as well as the maximum time measured are presented in Table I.

The results for more groups are similar. E.g. for the Modification of the Weighted Adjacency Matrix according to the rotor angle deviations, which is the most time-consuming part during real-time, an average time of 0.1453 s was measured with maximum time observed 0.2104 s for 4 groups. The simulations were carried out with an Intel® Core™2 Quad 2.83 GHz processor with 8 GB RAM.

Results demonstrating the performance of the proposed controlled islanding approach during disturbances will be presented in section IV-F. Statistical analysis of the overall performance is an objective for future work.

It is most likely that, after a disturbance, the islands formed with the controlled islanding have a load-generation imbalance, which cannot be compensated by the action of the primary frequency controllers. Therefore, under-frequency load shedding schemes must be utilized in order to stabilize the system. Such an approach is presented in the following.

TABLE I
COMPUTATION TIME OF REAL-TIME ALGORITHMS

	Average Time	Maximum Time
Off-line part		
Coherent Groups	1.501 s	1.9844 s
Real-time part		
Angles - Weight Mod.	0.1535 s	0.2099 s
Load-Gen Imbalance - Weight Mod.	0.031 s	0.040 s
k-means	0.0019 s	0.0152 s
Trip Lines Identification	0.0012 s	0.0119 s
Real-time Total	0.1876 s	0.277 s

III. Customer-Level Under-Frequency Load Shedding

In this section, the novel customer-level under-frequency load shedding (CL-UFLS) approach is introduced. After a brief review of conventional under-frequency load shedding (C-UFLS) approaches from literature, the motivation for a new system design is discussed and the necessary household infrastructure for implementing such a scheme is outlined. After that, some design principles and a concrete proposal of the information flow and the load shedding frequency threshold design is presented.

A. Review of Conventional Under-Frequency Load Shedding

Under-frequency load shedding is a long-known means to counteract a dangerous frequency decay in electric power systems and to restore the balance between load and generation in emergency situations. A number of load shedding methodologies from literature are mentioned in this section, which we will term C-UFLS techniques for the purpose of this paper.

Although there is a number of central load shedding approaches in which the loads are tripped based on the online minimization of an objective function as in [12], [13], most systems in use nowadays utilize under-frequency relays in substations which trip certain distribution feeders or entire transformers if an under-frequency situation is detected. Various methods for the decentralized measurement of the instantaneous power system frequency are available (see e.g. [14] for the commonly used Phase-Locked-Loop (PLL) measurement scheme, and [15] for a brief discussion of other available techniques and an extended PLL-based methodology). These techniques are implemented in a wide range of commercially available under-frequency relays.

The C-UFLS schemes implemented in different geographical regions are very diverse with respect to the handling of an under-frequency situation. The schemes may include only a measurement of the frequency f and the step-wise shedding of load according to a given stage plan (frequency steps) as outlined in [16]. A very common extension, often termed "adaptive UFLS", is the estimation of the frequency decay gradient df/dt in order to assess the lack of active power. See e.g. [17], [18], [19] for a discussion of such approaches.

B. Motivation and Idea of Customer-Level Load Shedding

In most of the load shedding schemes discussed above, the shedding action is implemented through frequency relays which trip entire distribution feeders in the case of a disturbance. The relays may be located on the lower-voltage side of the HV/MV transformers, or on subsequent MV/MV or MV/LV transformers in the distribution network. Thus, entire portions of the distribution network are de-energized by the trippings caused by the under-frequency relays. This means that the consumers on these feeders are not supplied with any electricity.

At the same time, all Distributed Generation (DG) units such as smaller wind farms, decentralized combined-heat-and-power (CHP) plants, or photovoltaic generation units on the shed feeders are lost. In the presence of high amounts of DG, the intended load shedding schemes can thus lead to significant involuntary generation shedding. This problem was described e.g. in [20]. Furthermore, the decision to trip a certain distribution feeder implies the shedding of a relatively large amount of power. This is due to the position of the load shedding relays, which is located on quite a high level in the vertical structure of the power system. If the location of the shedding action was more oriented towards the low-voltage side of the grid, i.e. closer to the customer level, this would allow for a more fine-tuned load reduction and the avoidance of over-shedding. At the same time, a higher number of frequency relays would have to be installed, which makes the system more expensive and possibly cumbersome to maintain.

One of the possible solution strategies is the migration of the shedding mechanism to the customer level utilizing two-way communication channels to individual appliances. This would allow to keep the distribution feeders energized and possibly installed DG units connected while minimizing the impact on the customer. First approaches to this issue exist in the literature [21]. Apart from under-frequency load shedding, the problem of under-voltage load shedding can also be regarded on the customer level, which is done in [22].

One important distinction has to be made with respect to frequency-dependent load control of consumer appliances. In the literature, there are numerous examples of the consideration of frequency-responsive cooling and heating loads which shall contribute to frequency stability. The original idea goes back to [23], where the term "FAPER" for such appliances was introduced. This idea has been picked up in a lot of current research such as [24], [25]. The operational behavior of such schemes is significantly different from the case considered here, although both deal with a customer-level frequency measurement and decentralized reaction. In the FAPER-like approaches, the control contribution comes from a frequency dead-band which works in both directions and is small enough to make an impact also for normal-operation frequency deviations. This is not the case in this setup, which is tailored for the rejection of larger disturbances without automatic re-activation after the shedding.

C. Household Infrastructure

The customer-level load shedding methodology utilizes a communication system which is usually referred to as "smart home" infrastructure [26]. The idea behind this concept is the connection of individual electric appliances on the consumers' premises via in-house communication networks. This provides novel functionalities for the customers, such as comfort and assistance features related to home automation, energy efficiency monitoring and visualization of domestic electricity consumption. An information gateway to the outside of the household can enhance comfort functionalities, e.g. by remote

control of home appliances. At the same time, sophisticated load management approaches requiring two-way communication are enabled. Novel business cases may be created by the electricity utilities, e.g. for control reserves provided by aggregated and coordinated groups of flexible household appliances [27]. Customer-level load shedding provides an additional benefit by increasing the security of supply whilst utilizing the same infrastructure.

While the idea of building automation is already very present in today's commercial and industrial facilities, home automation approaches have not yet managed to pass the threshold towards a mass implementation in consumer households. This is mainly due to high cost, lack of standardization and cumbersome installation and maintenance of in-house communication and control systems. However, recent developments show significant advances towards commercialization and mass implementation of home automation enabling technologies, e.g. powerline and wireless communication systems that can be integrated into home appliances, consume low amounts of power and may be produced in high quantities at low cost. These developments appear to support the idea of a future wide-spread implementation of "smart home" technologies.

D. System Design Principles

Several degrees of freedom exist in the design of the customer-level load shedding system. In a large power system with several million appliances spread throughout the system in individual households and commercial buildings, the flows of information have to be designed such that sensitive information is protected, the system is ensured to react as expected, clear advantages over more conventional approaches exist, and the operation is feasible from a practical point of view. These aspects are addressed by the following design principles which characterize the load shedding system developed in this work:

1) Non-transparency of the customer,
2) Centralized off-line computation, decentralized on-line disturbance reaction,
3) Category-wise appliance clustering,
4) Consideration of the "value of lost load" or similar ranking criteria,
5) Robustness towards varying system inertia,
6) Emulation of ramp-wise load shedding for smooth braking of the frequency decay.

Each of these points is justified and discussed with respect to its implications in the following.

1) Non-Transparency of the Customer: The first and obvious requirement established for the customer-level load shedding is that the customer should not lose privacy with respect to the possession and operation of appliances present on his or her premises. In fact, the adequate consideration of privacy concerns is recognized to be a major factor in the design of "smart home" and "smart grid" technologies [28]. This point is taken into account through the anonymous collection of aggregated data without the necessity to directly address and track individual households or even appliances.

2) Centralized Off-Line Computation, Decentralized On-Line Reaction: As a centralized triggering of shedding actions on individual consumers' premises may be too slow and unreliable for under-frequency load shedding, an autonomous reaction of the consumer loads is considered. It is assumed here that the system frequency can be measured locally in individual households and commercial companies by the in-house equipment, and shedding actions according to pre-set frequency thresholds can be triggered. As accurate rate-of-frequency measurements are quite costly, the customer-level load shedding system shall not rely on this information. Furthermore, it is clear that a 100 % system penetration with customer-level load shedding capability may take a long time to realize. Thus, the system has to be designed such that it can coexist with existing feeder-wise load shedding schemes.

3) Category-Wise Appliance Clustering: In order to avoid a high number of decision variables for the setting of frequency thresholds, the appliances should be clustered according to categories. Because of consumer-induced usage profiles, it appears practical to define the categories according to the function of the appliances. These categories account for specific portions of load during the day, which implies that the customer-level load shedding should be adaptable according to the load situation. Another advantage is that the value associated with operating these similar appliances at a specific time can be assumed approximately uniform. This implies a constant "value of lost load" for the appliances within the same category.

4) Consideration of the "Value of Lost Load": The "value of lost load" (VOLL) is a well-established term for the cost of a certain electricity outage. It is usually given in monetary units per kWh of energy not supplied to a customer. Different methodologies exist for such quantification, such as the assessment of costs through macro-economic modeling, surveys on the customers' directly incurred costs or on the willingness to pay for the avoidance of an outage, or empirical studies on the effects of major blackouts. Considering additionally the regional diversity of consumer structures and the usage of electricity, it is close to impossible to state universally applicable numerical values for outage costs. This argument is supported by the high diversity of VOLL assessments in the international literature, which is summarized in several surveys combining these results, e.g. [29], [30]. It can be seen that even the relation between residential and industrial load can be significantly different, as can be seen e.g. in [31] which states a relatively high value for the residential VOLL.

These findings suggest that, for the purpose of this paper, an assumption has to be made concerning the VOLL of different customer categories and load classes. This can be adapted towards more reality-based values when a more detailed study for a specific country shall be conducted. The concept shall be designed such that a change of VOLL assessments can easily be integrated into the system.

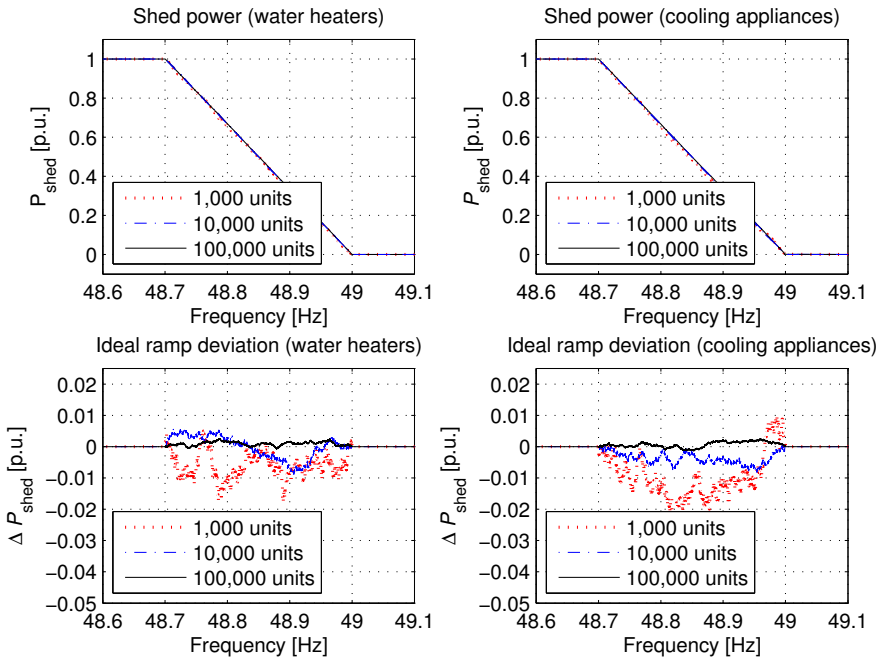

Fig. 3. Illustration of the effect of ramp-wise load shedding by assigning a random frequency threshold from a uniform distribution to individual units

5) Robustness towards Varying System Inertia: The splitting of a power system during a disturbance, as well as a high penetration of wind generators and inverter-connected DG, can lead to a significant reduction of the electromechanical inertia of the power system. Naturally, a very low inertia and the correspondingly higher volatility of the system frequency provides a challenge to any kind of under-frequency load shedding system which cannot detect the under-frequency situation and perform the tripping arbitrarily fast. However, the load shedding system should be designed such that a variable system inertia within reasonable bounds is not a major problem that would impede its effectiveness.

6) Emulation of Ramp-Wise Load Shedding: In the case of conventional under-frequency relays in substations, the reduction of system load has to be performed in a sequence of relatively large load steps. This is due to the amount of aggregated load behind a single frequency relay which can either be shed or not shed. However, when a frequency response mechanism is present on the appliance level, this can be exploited for a much smoother disturbance reaction. One way is the assignment of random frequency threshold values to all appliances within one class. In order to approximate a ramp-wise load reduction between two fixed frequency values, these random numbers should be generated from a uniform distribution between those boundaries.

Figure 3 illustrates the effect of uniformly distributed random values, in this case between 49 and 48.7 Hz (considering a nominal power system frequency of 50 Hz). In the left column, typical water heaters are considered as device category (equal shares of 2, 3, 4, 5, 6 kW rated power). In the right column, typical cooling appliances are shown (consisting of equal shares of 80, 90, 100, 110 and 120 W rated power). In both cases, the aggregation of 1,000, 10,000 and 100,000 units is considered. In the top plots, the shed power in per unit over the attained system frequency is illustrated. In the bottom plots, the deviation from an ideal ramp is shown, demonstrating the intuitive result that a better approximation is achieved by higher numbers of appliances. The maximum deviation of about 2 % for 1,000 appliances and much less than 1 % for 10,000 appliances and more shows that it is justified to consider the shedding by uniform random values approximately ramp-wise. Comparing the right and the left plots, it is apparent that the absolute power rating of the appliances is of low relevance for this matter.

E. Load Shedding Problem Formulation

In this section, the load shedding problem under consideration is formulated mathematically. The main goal is to describe both conventional load shedding based on frequency relays in distribution feeders, as well as the newly introduced customer-level load shedding of individual appliances, whilst taking into account the distribution of the load onto the network buses. For simplicity and transparency, all calculations related to load shedding are performed in MW instead of per unit. Note that we use 50 Hz as the nominal system frequency.

1) Power System Components: Considered is a power system consisting of several transmission lines which interconnect a number of buses with attached central generators and distribution feeders. These feeders can be considered a model for ”portions” of load that can be disconnected by a single frequency relay. I.e., if the shedding in the underlying distribution system is realized by the tripping of entire MV/MV or MV/LV transformers, these can also be described as feeders because the distribution network structure is not modeled for the purposes of this paper.

Apart from the feeder subdivision, the load at each bus can be subdivided into load classes according to the associated functions that the load fulfills (such as cooking, washing, freezing, etc.). In this formulation, the load classes constitute a categorization which is distinct from the distribution feeder subdivision. As the former is a customized categorization while the latter represents the physical structure of the system, the load classes can be considered to be distributed onto the individual feeders as well. This is illustrated in Fig. 4.

Equations (11) – (13) show the nomenclature for the buses n, the load classes i_n, and the feeders j_n at bus n:

$$\text{Bus: } n \in \mathfrak{N} = \{1, \ldots, N\}, \quad (11)$$

$$\text{Load class at bus } n\text{: } i_n \in \mathfrak{L}_n = \{1, \ldots, N_{\mathrm{L}_n}\}, \quad (12)$$

$$\text{Distr. feeder at bus } n\text{: } j_n \in \mathfrak{F}_n = \{1, \ldots, N_{\mathrm{F}_n}\}. \quad (13)$$

For simplicity, the load classes are defined independently of the buses, so the number of load classes N_{L_n} is equal for all n and they represent the same kind of load (e.g. residential cooling load). Note that this does not imply that all load classes have to be actually present at all buses.

2) Load Ratios: The load at bus n, $P_{\mathrm{L},n}$, can be modeled by commonly used aggregated load models for power system studies, e.g. as found in [32]. In principle, each feeder and load class could be represented by a different load model according to its characteristics, although this might only be needed for a very detailed study of a specific system. In this paper, we will represent the load at one bus by the same model. As the load shedding system will act independently of the load dynamics, the static load $P_{\mathrm{L0},n}$ at bus n is considered for the computations. The same holds for the load classes and the feeder loads, as stated below.

For the subdivision of $P_{\mathrm{L0},n}$ into load classes P_{L0,i_n}, it is practical to define the ratios r_{L,i_n} between the individual load classes i on bus n and the total bus load. The load distribution onto the different feeders j at bus n is handled in the same way:

$$r_{\mathrm{L},i_n} = P_{\mathrm{L0},i_n}/P_{\mathrm{L0},n} \quad , \quad (14)$$

$$r_{\mathrm{F},j_n} = P_{\mathrm{F0},j_n}/P_{\mathrm{F0},n} \quad . \quad (15)$$

In order to render the notation more compact, these ratios can be written as ratio vectors for each bus n in the system, the 1-norm of which has to be equal to 1 by definition:

$$\mathbf{r}_{\mathrm{L},n} = [r_{\mathrm{L},1_n}, \ldots, r_{\mathrm{L},N_{L_n}}]^{\mathrm{T}} \quad , \quad (16)$$

$$\mathbf{r}_{\mathrm{F},n} = [r_{\mathrm{F},1_n}, \ldots, r_{\mathrm{L},N_{F_n}}]^{\mathrm{T}} \quad . \quad (17)$$

In the case of the customer-level load shedding, one further detail has to be considered: The total penetration of the customer-level load shedding system into a certain appliance class may be much less than 100 % (for instance, only half of the refrigerators in a country could be equipped with the household load shedding capability). For this reason, the penetration ratio $r_{\mathrm{pen},i_n} \in [0, 1]$ is defined, which indicates the ratio of appliances in a class equipped with customer-level load shedding capability. This can also be gathered in the vector

$$\mathbf{r}_{\mathrm{pen},n} = [r_{\mathrm{pen},1_n} \ldots r_{\mathrm{pen},N_{L_n}}]^{\mathrm{T}} \quad . \quad (18)$$

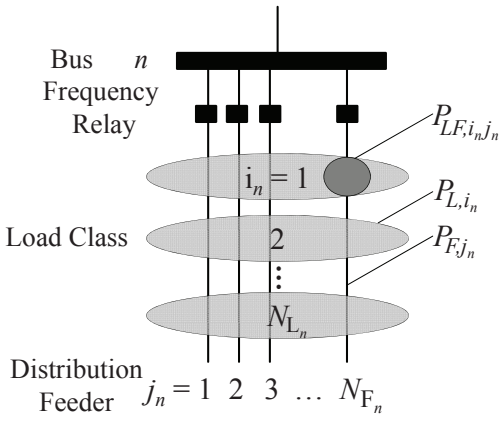

Fig. 4. Feeders and load classes at an arbitrary bus n

The load shedding system penetration is assumed to be uniform throughout the system, i.e. $\mathbf{r}_{\mathrm{pen},n}$ is equal for all n.

F. Load Shedding System Layout and Flow of Information

Based on the design principles outlined above, a concrete implementation of the customer-level load shedding system can be described and the flow of information can be determined. The communication system needed for implementing the scheme under consideration may run on a variety of hardware platforms. It has to support the following characteristics:

I) Assignment of a random frequency threshold to each individual appliance based on a uniform probability distribution determined by the load shedding system administrator, e.g. grid control center. This requires the clustering of appliances according to their load class (e.g. stoves, refrigerators, lighting, etc.). Essentially, the vectors $\mathbf{r}_{\mathrm{L},n}$ and $\mathbf{r}_{\mathrm{F},n}$ as described in equations (16) and (17) have to be obtained from aggregated measurements or estimations.

II) Decentralized measurement of the power system frequency on the household level. This can be performed either in the individual appliances or in the customer's switchboard.

III) Comparison of the currently measured power system frequency with the assigned threshold (including a delay for secure detection) and triggering of the disconnection of the appliance in case of a system frequency below the threshold value.

The conventional load shedding is assumed to stay in place and has to exhibit almost the same characteristics (with the exception that the thresholds are not derived from a probability distribution).

Figure 5 depicts the flow of information between the load shedding administrator and the units. The information obtained from the units and the subsequent assignment of the conventional load shedding thresholds $f^{\mathrm{fr}}_{\mathrm{thr},j_n}$ is visualized, as well as the customer-level thresholds $f^{\mathrm{cl,1}}_{\mathrm{thr},i_n}$ and $f^{\mathrm{cl,2}}_{\mathrm{thr},i_n}$, which are the boundaries of the uniform distribution from which the

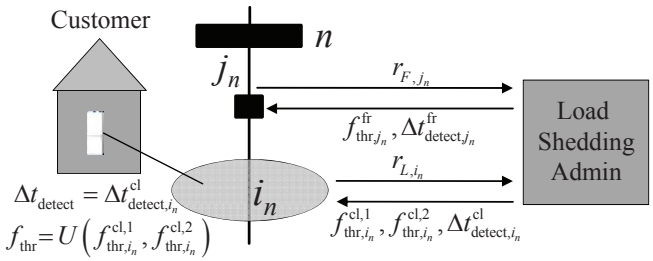

Fig. 5. Flow of information between the load shedding administrator and the units

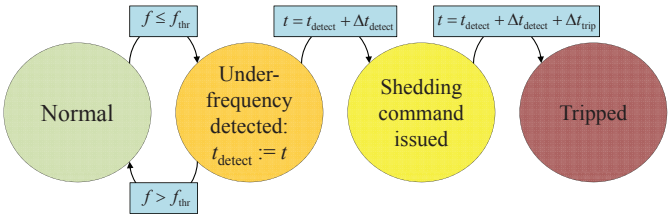

Fig. 6. Finite state machine of load shedding mechanism, valid for both the conventional load shedding relays in the distribution feeders and the customer-level load shedding relays contained in individual appliances

individual appliance thresholds are taken (cf. section III-D6). The time delays $\Delta t^{\mathrm{fr}}_{\mathrm{detect},j_n}$ and $\Delta t^{\mathrm{cl}}_{\mathrm{detect},i_n}$ are further design parameters, which is explained in the next sections.

1) Conventional Load Shedding: The conventional load shedding system is composed of frequency relays (denoted by superscript fr) assumed to be present in every distribution feeder of the entire system. An arbitrary relay on feeder j_n at bus n is characterized by three parameters: the threshold frequency $f^{\mathrm{fr}}_{\mathrm{thr},j_n}$, the detection time delay $\Delta t^{\mathrm{fr}}_{\mathrm{detect},j_n}$ and the tripping time delay $\Delta t^{\mathrm{fr}}_{\mathrm{trip},j_n}$. In case an under-frequency situation is detected, the shedding command is issued after $\Delta t^{\mathrm{fr}}_{\mathrm{detect},j_n}$ has passed and the measured frequency f_n did not return above the threshold. Once the shedding command has been issued, the actual tripping is performed after $\Delta t^{\mathrm{fr}}_{\mathrm{trip},j_n}$. The behavior of the frequency relay can be illustrated by the finite state machine shown in Fig. 6.

We define now the remaining load at one feeder as the difference of the load before the shedding and the shed load:

$$P_{\mathrm{F0,rem},j_n} = P_{\mathrm{F0},j_n} - P_{\mathrm{F0,shed},j_n} \quad . \tag{19}$$

Corresponding to the load class and feeder ratios defined above, the shedding ratio of the feeder j_n is defined as the relation of the currently shed load value to the value before the shedding:

$$r^{\mathrm{fr}}_{\mathrm{shed},j_n} = P_{\mathrm{L0,shed},j_n} / P_{\mathrm{L0},j_n} \quad . \tag{20}$$

As a single feeder is either shed or not shed, $r_{\mathrm{shed},j_n} \in \{0,1\}$ must hold. The following equations describe the logic of the shedding, taking into account the theoretical shedding (theo) which would be caused in the case of instantaneous shedding, the shedding if only detection time delay was considered (detect), and the true shedding including the tripping delay:

$$r^{\mathrm{fr,theo}}_{\mathrm{shed},j_n}(t) = \begin{cases} 0 & \text{for } f_n(t) > f^{\mathrm{fr}}_{\mathrm{thr},j_n} \\ 1 & \text{for } f_n(t) \le f^{\mathrm{fr}}_{\mathrm{thr},j_n} \end{cases} , \tag{21}$$

$$r^{\mathrm{fr,detect}}_{\mathrm{shed},j_n}(t) = r^{\mathrm{fr,theo}}_{\mathrm{shed},j_n}\Big(\max_{\tilde{t}\in[t-\Delta t^{\mathrm{fr}}_{\mathrm{detect},j_n},t]} f_n(\tilde{t})\Big) , \tag{22}$$

$$r^{\mathrm{fr}}_{\mathrm{shed},j_n}(t) = r^{\mathrm{fr,detect}}_{\mathrm{shed},j_n}(t - \Delta t_{\mathrm{trip},j_n}) \quad . \tag{23}$$

Having established the requirement that the load should not be reactivated automatically once the frequency returns above the threshold, the shedding ratio is restricted to be monotonically increasing, i.e. for the time instants t_1 and t_2 with $t_1 \le t_2$ holds

$$r^{\mathrm{fr}}_{\mathrm{shed},j_n}(t_1) \le r^{\mathrm{fr}}_{\mathrm{shed},j_n}(t_2) \quad . \tag{24}$$

The main design parameters for the load shedding system are thus the frequency thresholds and the detection time delays of the frequency relays. The tripping time delay represents the latency of the frequency relay and can only be influenced by alteration of the tripping mechanism.

2) Customer-Level Load Shedding: The shedding ratios of the customer-level load shedding (denoted by superscript cl) are determined as follows: based on the ramp-wise load shedding emulation outlined in section III-D6, two frequency thresholds have to be given to each load class. The actual threshold of each appliance is then determined on the household level. In an analogous way to the conventional load shedding, we define the shed and remaining load caused by one load class i_n at bus n, as well as the shedding ratio:

$$P_{\mathrm{L0,rem},i_n} = P_{\mathrm{L0},i_n} - P_{\mathrm{L0,shed},i_n} \quad , \tag{25}$$

$$r^{\mathrm{cl}}_{\mathrm{shed},i_n} = P_{\mathrm{L0,shed},i_n} / P_{\mathrm{L0},i_n} \quad . \tag{26}$$

As the load shedding is performed ramp-wise, $r_{\mathrm{shed},j_n} \in [0,1]$ holds in contrast to the conventional load shedding. The following equations describe the logic of the shedding, taking into account the theoretical shedding (theo) which would be caused in the case of instantaneous shedding, the shedding if only detection time delay was considered (detect), and the true shedding including the tripping delay:

$$r^{\mathrm{cl,theo}}_{\mathrm{shed},i_n}(t) = \begin{cases} 0 & \text{for } f_n(t) > f^{\mathrm{cl},1}_{\mathrm{thr},i_n} \\ r_{\mathrm{pen},i_n} \frac{f^{\mathrm{cl},1}_{\mathrm{thr},i_n} - f_n}{f^{\mathrm{cl},1}_{\mathrm{thr},i_n} - f^{\mathrm{cl},2}_{\mathrm{thr},i_n}} & \text{for } f^{\mathrm{cl},2}_{\mathrm{thr},i_n} < f_n(t) \le f^{\mathrm{cl},1}_{\mathrm{thr},i_n} \\ r_{\mathrm{pen},i_n} & \text{for } f_n(t) \le f^{\mathrm{cl},2}_{\mathrm{thr},i_n} \end{cases} , \tag{27}$$

$$r^{\mathrm{cl,detect}}_{\mathrm{shed},i_n}(t) = r^{\mathrm{cl,theo}}_{\mathrm{shed},i_n}\Big(\max_{\tilde{t}\in[t-\Delta t^{\mathrm{cl}}_{\mathrm{detect},i_n},t]} f_n(\tilde{t})\Big) , \tag{28}$$

$$r^{\mathrm{cl}}_{\mathrm{shed},i_n}(t) = r^{\mathrm{cl,detect}}_{\mathrm{shed},i_n}(t - \Delta t^{\mathrm{cl}}_{\mathrm{trip},i_n}) \quad . \tag{29}$$

Same as in the case of conventional load shedding, the shedding ratio is restricted to be monotonically increasing, i.e. for the time instants t_1 and t_2 with $t_1 \le t_2$ holds

$$r^{\mathrm{cl}}_{\mathrm{shed},i_n}(t_1) \le r^{\mathrm{cl}}_{\mathrm{shed},i_n}(t_2) \quad . \tag{30}$$

3) Remaining Load at Bus n: Any combination of the previously modeled C-UFLS system and the newly introduced CL-UFLS system has to take into account the fact that the same load can only be tripped once. Thus, the effects of both load shedding systems have to be concatenated. This requires one further assumption, namely the distribution of

one individual load class at one bus onto the feeders at this bus. It is assumed here that a certain load class P_{L,i_n} at bus n is equally distributed onto the N_{F_n} feeders at this bus, i.e.

$$P_{\mathrm{LF},i_n j_n} = P_{\mathrm{L},i_n}/N_{\mathrm{F}_n} \quad \forall i_n \in \mathfrak{L}_n, j_n \in \mathfrak{F}_n \quad . \tag{31}$$

Under this requirement, the concatenation of customer-level and conventional load shedding is performed in the following way: the remaining load at the bus due to a certain customer-level load shedding ratios $\mathbf{r}_{\mathrm{L},n}$ is calculated, which is then subject to a further reduction by the conventional load shedding ratio $\mathbf{r}_{\mathrm{F},n}$. The remaining load after the customer-level load shedding is described by

$$P^{\mathrm{cl}}_{\mathrm{L0,rem},n} = \mathbf{r}^{\mathrm{T}}_{\mathrm{L},n}\left[\mathbf{1} - \mathbf{r}^{\mathrm{cl}}_{\mathrm{shed},n}\right] P_{\mathrm{L0},n} \quad . \tag{32}$$

The effect of the conventional load shedding is independent of the class-dependent load reduction because of the requirement from equation (31). Thus, it can be assumed to act on the aggregated remaining load after the customer-level load shedding:

$$P^{\mathrm{fr}}_{\mathrm{L0,rem},n} = \mathbf{r}^{\mathrm{T}}_{\mathrm{F},n}\left[\mathbf{1} - \mathbf{r}^{\mathrm{fr}}_{\mathrm{shed},n}\right] P^{\mathrm{cl}}_{\mathrm{L0,rem},n} \quad . \tag{33}$$

Inserting equation (32) into (33), the remaining load at bus n is equal to:

$$P_{\mathrm{L0,rem},n} = \mathbf{r}^{\mathrm{T}}_{\mathrm{F},n}[\mathbf{1} - \mathbf{r}^{\mathrm{fr}}_{\mathrm{shed},n}] \cdot \mathbf{r}^{\mathrm{T}}_{\mathrm{L},n}[\mathbf{1} - \mathbf{r}^{\mathrm{cl}}_{\mathrm{shed},n}] P_{\mathrm{L0},n} \quad . \tag{34}$$

G. Frequency Threshold Pre-Computation

In this section, the frequency threshold computation will be presented both for the conventional and the customer level load shedding.

1) Conventional Load Shedding: In this work, we consider a load shedding stage plan as commonly used in the ENTSO-E Continental Europe region [16]. It will consist of four load shedding stages defined by the thresholds $f^{\mathrm{fr}}_{\mathrm{stage1}}, \ldots, f^{\mathrm{fr}}_{\mathrm{stage4}}$ and the detection time delays $\Delta t^{\mathrm{fr}}_{\mathrm{detect,\ stage1}}, \ldots, \Delta t^{\mathrm{fr}}_{\mathrm{detect,stage4}}$. The tripping time delays $\Delta t^{\mathrm{fr}}_{\mathrm{trip}}$ are assumed to be given by the frequency relays in use.

We take the following simple approach for parameterizing the conventional load shedding system: The stages are selected heuristically, roughly based on the recommendations set forth in [16]. The distribution of the frequency thresholds onto all feeders in the system is then performed in the following way:

1) Select the current load shedding stage $k \in \{1 \ldots 4\}$,
2) Assign randomly selected feeders to the k^{th} load shedding stage (frequency threshold and detection time) until the shed power at stage k is corresponding to the stage plan requirement,
3) Progress to the next load shedding stage until a sufficient amount of feeders has been assigned to each stage.

2) Customer-Level Load Shedding: Having established the appliance categories for a given system, the associated frequency thresholds must be determined. As stated before, the threshold tuning should take into account the "value of lost load" of load class i_n at bus n, denoted by $VOLL_{i_n}$, or by the vector $\mathbf{VOLL}_n$. As stated in section III-E1, the load classes i_n are defined identically for all n, and thus $\mathbf{VOLL}_n$ is identical for all n.

Optimization-based tuning methods can be used in order to find the frequency thresholds $f^{\mathrm{cl},1}_{\mathrm{thr},i_n}$ and $f^{\mathrm{cl},2}_{\mathrm{thr},i_n}$. In order to reduce the complexity of this work, we choose a simple method that considers the VOLL while ensuring a constant relation between shed load and system frequency for the entire frequency span of the customer-level load shedding. The following algorithm is used:

1) Determine the frequency span of the customer-level load shedding: it should not start above a certain minimum deviation of the frequency from its nominal value, e.g. $f^{\mathrm{cl},1}_{\mathrm{thr,max},i_n} = 48.8$ Hz, in order to avoid activation in normal operation situations. We define furthermore that the customer-level load shedding should end before the first conventional load shedding stage with a certain margin, e.g. $f^{\mathrm{cl},2}_{\mathrm{thr,min},i_n} = f^{\mathrm{fr}}_{\mathrm{thr,max},j_n} + 0.2$ Hz.
2) Calculate the aggregated shedding slope

$$m_{\mathrm{agg}} = \Delta P^{\mathrm{cl}}_{\mathrm{L,total}}/\Delta f^{\mathrm{cl}}_{\mathrm{total}} \ [\mathrm{MW/Hz}] \quad , \tag{35}$$

with the total power $\Delta P^{\mathrm{cl}}_{\mathrm{L,total}} = \sum_{n=1}^{N} \mathbf{r}^{\mathrm{T}}_{\mathrm{pen},n}\mathbf{r}_{\mathrm{L},n}P_{\mathrm{L},n}$ and the frequency span $\Delta f^{\mathrm{cl}}_{\mathrm{total}} = f^{\mathrm{cl},1}_{\mathrm{thr,max},i_n} - f^{\mathrm{cl},2}_{\mathrm{thr,min},i_n}$.
3) Sort the appliance categories according to the vector $\mathbf{VOLL}_n$ in ascending order. This defines the shedding sequence of the individual categories with decaying frequency.
4) Calculate for each load class the frequency span such that the shedding slope of the load class is equal to aggregated shedding slope: $m_i = m_{\mathrm{agg}}$, where m_i is calculated for class i in an analogous way to m_{agg} in equation (35).

A graphic illustration of this approach is given in section IV-D2. It is further determined that the detection time delays are set to identical values for all classes. The selected value depends on the transient behavior of the used power system frequency measurement system.

After having introduced the customer-level load shedding, it can be seen that the amount of power shed by the conventional load shedding system is different. This is due to the fact that the shed feeders have a lighter loading because part of the load is already off. Depending on the system penetration of the customer-level load shedding, the conventional load shedding system settings can be adapted. This is illustrated in section IV-D2.

IV. Case Study

In order to demonstrate the effectiveness of the approaches presented above, time-domain simulations are conducted using the IEEE 118-bus system. After introducing four simulation scenarios, the power system model, the islanding and load shedding parameterizations, as well as the considered disturbance, the simulation results will be presented and discussed.

TABLE II
DYNAMIC PARAMETERS OF THE GENERATORS

Gen. No.	S_r [MVA]	V_r [kV]	H [s]	x'_d [p.u.]	K_D [MW/Hz]
10	512	24	2.63	0.27	12
12	100	13.8	4.99	0.06	12
25	270	18	4.13	0.256	12
26	384	24	2.62	0.324	12
31	9	6.9	2.61	0.408	12
46	35	13.8	7.26	0.26	12
49	250	18	6.41	0.195	12
54	65.8	13.8	2.67	0.26	12
59	192	18	3.3	0.232	12
61	192	18	3.3	0.232	12
65	448	22	2.66	0.265	12
66	448	22	2.66	0.265	12
69	590	22	2.32	0.28	12
80	590	22	2.32	0.28	12
87	9	6.9	2.61	0.408	12
89	835	20	2.64	0.413	12
100	270	18	4.13	0.256	12
103	52.2	13.8	4.98	0.209	12
111	52.2	13.8	4.98	0.209	12

TABLE III
PARAMETERS OF TURBINE AND REGULATORS

Governor and turbine parameters

R	TS	TC	$T3$	$T4$	$T5$
0.04	20	0.2	0.2	0.2	0.2

AVR parameters

V_set	T_R	K_a	T_a	T_b	T_c	EFD_max	EFD_min
1	0.02	200	0.015	10	1	5	-5

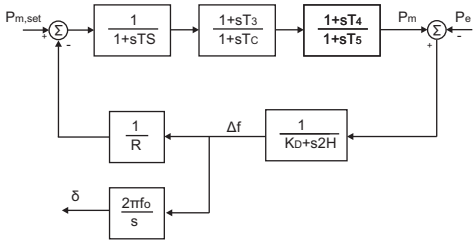

Fig. 8. Generator frequency dynamics

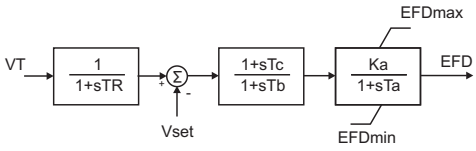

Fig. 9. AVR block diagram

A. Simulation Scenarios

For a line fault disturbance that is able to generate an angular instability situation, the following cases will be shown:

- C1 Frequency response without controlled islanding and with conventional load shedding only,
- C2 Frequency response with controlled islanding and conventional load shedding only,
- C3 Frequency response with controlled islanding and customer-level load shedding, where the conventional load shedding system remains unchanged,
- C4 Frequency response with controlled islanding and customer-level load shedding, with adaptation of the conventional load shedding system.

The selected cases serve to evaluate the proposed methods in the order of increasing complexity. It will be shown that each further case is more effective in mitigating the disturbance than the preceding one.

B. Power System Model

As stated above, the performance of the proposed approach is evaluated on the IEEE 118-bus network which is considered complex enough to capture the difficulties that may arise in the real system. The data of the model are retrieved from a snapshot available at [11]. It includes 19 generators, 177 lines, 99 load buses and 7 transmission level transformers. The system used in the simulations contains slight modifications so as to render the model in a more realistic configuration. Thus in order to represent the different voltage levels, 19 more transformers are added to connect the medium-voltage generator buses (6.9 – 24 kV) with the high voltage transmission level buses (400 kV). Moreover, since there were no dynamic data available, typical values provided by [33] were used for the simulations. Figure 7 shows a single-line diagram of the network.

All generators are represented by the classical model and are also equipped with primary frequency control and Automatic Voltage Regulator (AVR). Figure 8 depicts the block diagram of the interaction between the turbine, the primary frequency control and the generator frequency dynamics that was used for each generator. $P_\mathrm{m,set}$ is the scheduled power generation, P_m is the mechanical power that serves as an input to the generator and P_e is the electric power which is absorbed by the network. The simplified AVR model is illustrated in Fig. 9, where V_T is the voltage magnitude at the output of the generator, V_set is the setpoint of that voltage and EFD represents the field voltage. All variables are in p.u.

The dynamic data used in the simulations are summarized in Tables II and III. The setpoint of the scheduled mechanical power ($P_\mathrm{m,set}$) of each generator is determined according to the mentioned IEEE 118-bus system power flow case.

The load model for the load at bus n, $P_{\mathrm{L},n}$, implies a voltage dependency of the load, while a frequency dependency is not considered:

$$P_{\mathrm{L},n} = P_{\mathrm{L0},n}(V_T/V_0)^\alpha, \tag{36}$$

$$Q_{\mathrm{L},n} = Q_{\mathrm{L0},n}(V_T/V_0)^\beta. \tag{37}$$

The exponents α and β are set both equal to 2 representing constant impedance characteristics.

The model of the network is implemented using NEPLAN® [34], a power system dynamic simulator which is suitable for transient stability analysis. In order to interact with the system during run-time using customized algorithms, the NEPLAN® model was converted to a dynamic simulation environment for MATLAB® [35].

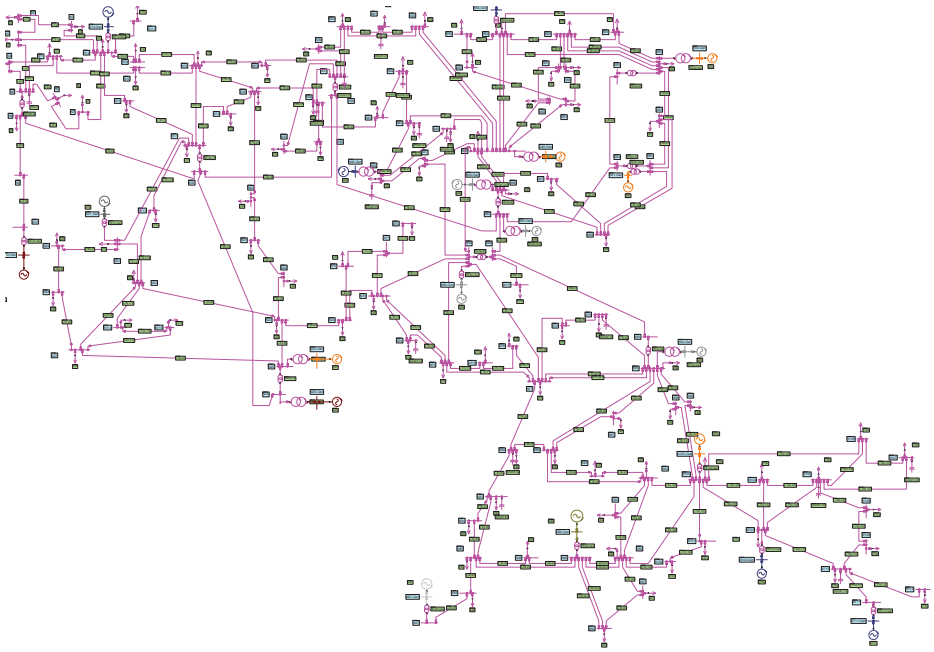

Fig. 7. Topology of the IEEE 118-bus system

TABLE IV
COHERENT GROUPS OF GENERATORS

	Generator Buses
Group 1	46, 49, 80, 89
Group 2	66, 87, 100, 103, 111
Group 3	10, 12, 25, 26, 31, 54, 59, 61, 65, 69

TABLE V
CONVENTIONAL LOAD SHEDDING STAGE PLAN

$f_{\text{thr}}^{\text{fr}}$	$\Delta t_{\text{detect}}^{\text{fr}}$	$\Delta t_{\text{trip}}^{\text{fr}}$	$P_{\text{F,shed}}^{\text{fr}}/P_{\text{F}}^{\text{fr}}$
49.0 Hz	0.10 s	0.05 s	15.00 %
48.7 Hz	0.10 s	0.05 s	15.00 %
48.4 Hz	0.10 s	0.05 s	15.00 %
48.1 Hz	0.10 s	0.05 s	15.00 %

C. Controlled Islanding Pre-Computations

For the purpose of this paper, the 3 slowest modes are selected and, according to the Slow Coherency algorithm, the generators are partitioned into 3 coherent groups, as shown in Table IV. The rest of the computations take place in real-time right after the detection of the disturbance.

D. Load Shedding System Parameterization

Both load shedding systems are parameterized according to the methodologies stated in section III-G. Note that the detection time delays are set to a uniform value, which is adapted to the transient behavior of the instantaneous bus frequency measurement realized by a Phase-Locked-Loop (PLL) system.

1) Conventional Load Shedding: For a specific load situation, the load at each bus of the system is known. For the purpose of parameterizing the load shedding system, distribution feeders have to be artificially created as they are not part of the available data. As already stated above, the feeders represent only portions of load to be disconnected in one piece since the distribution system topology is not modeled. Therefore, we take a simple approach which creates a reasonably realistic number of feeders and distribution of load:

First, the cumulated active power load in the whole system is compared with the cumulated active power limits of the generators, which yields the current load factor of the entire system. By proportional scaling, the load at each bus is adapted such that the system is at maximum loading. Based on this, the number of feeders at each bus is determined by assuming a maximum feeder capacity. We assume a maximum of 20 MW per feeder, and consequently end up with a varying number of feeders at different buses in the range between 1 and 20.

Now, the load at each bus of the unscaled system (original load situation) is distributed with some stochastic variability (scaling factors from a normal distribution with mean 1 and 20 % standard deviation) onto the feeders. The last feeder at one bus has to take the remainder of the load, such that the original bus load is not changed. Figure 10 shows the load per feeder, clustered by the corresponding buses. Note that the feeder load can be slightly higher than the established maximum of 20 MW because of the stochastic load assignment to the feeders, which is a case that can also temporarily occur in reality.

The parameters for the conventional load shedding are based on the stage plan presented in Table V.

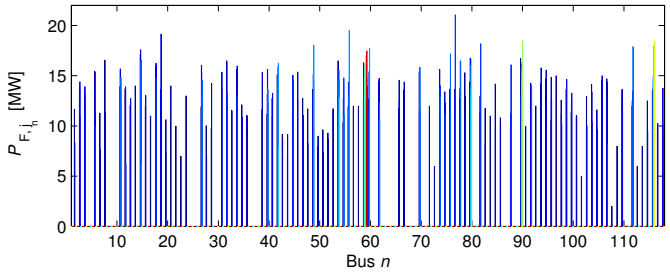

Fig. 10. Distribution of load onto the distribution feeders

TABLE VI
ASSUMED CUSTOMER CATEGORIES IN 118-BUS SYSTEM

Customer Category	Region 1	Region 2	Region 3
Residential	70.00 %	20.00 %	50.00 %
Industrial	20.00 %	70.00 %	10.00 %
Commercial	10.00 %	10.00 %	40.00 %
Bus numbers belonging to cat.	1 – 33; 113 – 115; 117	34 – 74; 116	75 – 112; 118

2) Customer-Level Load Shedding: In order to parameterize the customer-level load shedding, the load classes have to be created first. In this present work, this is entirely assumption-based, however reasonably realistic. In a first step, the 118-bus system is divided in three regions, which are assumed to have different compositions of customer categories (residential, commercial, industrial). The assumed shares of each customer category in the regions is summarized in Table VI.

The customer categories are now subdivided into subcategories, the total set of which constitutes the load classes for the customer-level load shedding. In Table VII, the 14 load classes created for the present system are summarized. In the column "Rel. Share", the percentage is stated that the load class accounts for with respect to its customer category. This is actually only valid for one specific load situation, and will consequently vary during the course of the day. Based on the calculations performed in this paper, a category-wise load profile can easily be used for the creation of time-dependent frequency threshold assignments. For details on the time-varying load shedding potential of residential customers with exemplary calculations for Germany, see [36].

Assumptions for the "value of lost load" per customer category are shown in the colum "VOLL(category)". Note that the VOLL value is expressed in EUR/kWh of energy not supplied – which means that a certain load shedding action has to be combined with an assumed outage duration in order to yield a monetary value. We assume this to be 1 hour for the load shedding actions that are performed in the presently simulated cases. This may be exaggerated in the case of smaller-scale shedding actions. However, in case of larger disturbances causing under-frequency situations in the entire system, the actual outage duration will probably be higher. For a direct comparability of the results, the VOLL value should be calculated by estimated outage durations based on the magnitude of the disturbance. This, however, is beyond the scope of this paper.

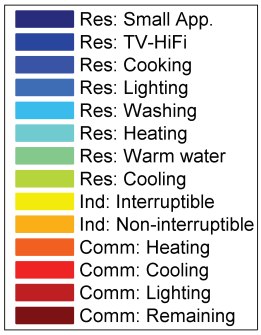

Fig. 11. Legend of the load classes for load shedding plots

As further presented in Table VII, a VOLL modifier is introduced in order to rank the customer comfort loss brought about by the disconnection of specific appliance types. With this, the modified VOLL(class) is derived. Next to this column, the assumptions about customer-level load shedding penetration are summarized, which is a moderate 50 % for selected appliance types in the present case. The frequency thresholds $f_{\mathrm{thr},i_n}^{\mathrm{cl},1}$ and $f_{\mathrm{thr},i_n}^{\mathrm{cl},2}$ are calculated based on the algorithm presented in section III-G. Finally, the load shedding time delays are stated (identical detection time related to measurement transients, shedding-system-related tripping time).

Now the load shedding system performance is analyzed by a static calculation of the remaining load according to system frequency. This is done for the simulated Cases 1 and 2, Case 3, and Case 4. The main purpose of this calculation is to gain an understanding of the interaction between the customer-level and the conventional load shedding system, which influence each other in spite of the fact that they operate in different frequency ranges. Note that this influence does not occur in operational terms, but rather due to the two shedding systems operating on the same loads.

Figures 12, 13 and 14 depict the remaining system load according to bus in MW (top plot), the shed load according to load class (middle plot) and the cumulated VOLL according to class (bottom plot). For the plots referring to load classes, the legend presented in Fig. 11 holds. It is important to note that in Fig. 13 the conventional load shedding is impacted in two ways: first, the actual system load is less than what the conventional load shedding was designed for: in fact, the first shedding stage of the stage plan has already been fulfilled before even reaching it. The second effect is that the shed load per stage is reduced, as part of the load on the shed feeders is already off. These effects can be desirable or not. If a performance of the system with customer-level load shedding similar to the conventional system is desired, this can be achieved by adapting the frequency thresholds of the conventional load shedding as shown in Fig. 14. In this case, the first load shedding stage is completely eliminated, and the others are just adapted by some percent in order to meet the thresholds stipulated in the stage plan.

TABLE VII
LOAD CLASSES, ASSUMED VOLL AND FREQUENCY THRESHOLDS

Category	Class	Rel. Share	VOLL(category)	Modifier	VOLL(class)	$r^{\mathrm{cl}}_{\mathrm{pen},i_n}$	$f^{\mathrm{cl},1}_{\mathrm{thr},i_n}$	$f^{\mathrm{cl},2}_{\mathrm{thr},i_n}$	$\Delta t^{\mathrm{cl}}_{\mathrm{detect},i_n}$	$\Delta t^{\mathrm{cl}}_{\mathrm{trip},i_n}$
Residential	Small Devices	23 %	15 EUR/kWh	2	30 EUR/kWh	0 %	–	–	–	–
Residential	TV-HiFi	7 %	15 EUR/kWh	2	30 EUR/kWh	0 %	–	–	–	–
Residential	Cooking	10 %	15 EUR/kWh	1	15 EUR/kWh	0 %	–	–	–	–
Residential.	Lighting	9 %	15 EUR/kWh	2	30 EUR/kWh	0 %	–	–	–	–
Residential	Washing	12 %	15 EUR/kWh	1	15 EUR/kWh	50 %	49.1962	49.1000	0.1 s	0.1 s
Residential	Heating	3 %	15 EUR/kWh	0	0 EUR/kWh	50 %	49.8000	49.7760	0.1 s	0.1 s
Residential	Warm water	14 %	15 EUR/kWh	0	0 EUR/kWh	50 %	49.7760	49.6637	0.1 s	0.1 s
Residential	Cooling	22 %	15 EUR/kWh	0	0 EUR/kWh	50 %	49.6637	49.4874	0.1 s	0.1 s
Industrial	Interruptible	10 %	25 EUR/kWh	0	0 EUR/kWh	50 %	49.4874	49.4488	0.1 s	0.1 s
Industrial	Non-interr.	90 %	25 EUR/kWh	2	50 EUR/kWh	0 %	–	–	–	–
Commercial	Heating	20 %	30 EUR/kWh	0	0 EUR/kWh	50 %	49.4488	49.3044	0.1 s	0.1 s
Commercial	Cooling	15 %	30 EUR/kWh	0	0 EUR/kWh	50 %	49.3044	49.1962	0.1 s	0.1 s
Commercial	Lighting	15 %	30 EUR/kWh	1	30 EUR/kWh	0 %	–	–	–	–
Commercial	Remaining	50 %	30 EUR/kWh	3	90 EUR/kWh	0 %	–	–	–	–

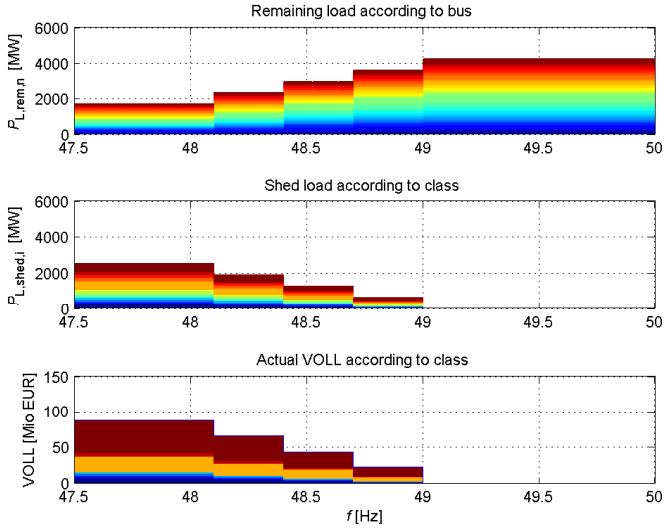

Fig. 12. Static analysis of the load shedding system – conventional only

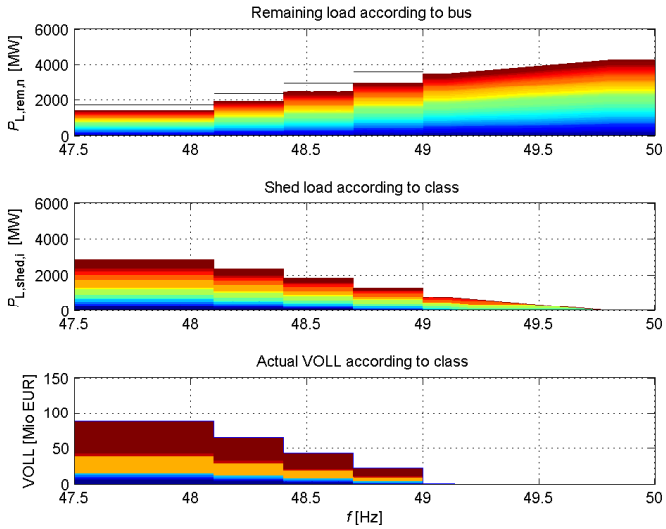

Fig. 13. Static analysis of the load shedding system – CL-UFLS with unchanged C-UFLS

E. Disturbance Scenarios

Disturbances that lead to angle instability are very likely to bring the system to a state of cascading failures, since it is very difficult to treat these disturbances with the common emergency control strategies that rely mainly on devices reacting to local measurements. Hence, any disturbance that may lead to loss of synchronism between the generators constitutes a scenario that highlights the necessity of the controlled islanding scheme, which considers the status of the whole network. Line faults can lead to this kind of instability.

After an exhaustive search of the possible fault scenarios, considering one or two lines, a scenario was chosen which we believe illustrates clearly the benefits of the proposed approach. This scenario consists of a fault on lines 100-103 and 100-104 on the side of bus 100. The fault occurs at $t = 0.1$ s, and after 0.15 s it is cleared by local line protections (i.e. the lines between the buses 100-103 and 100-104 are tripped at $t = 0.25$ s).

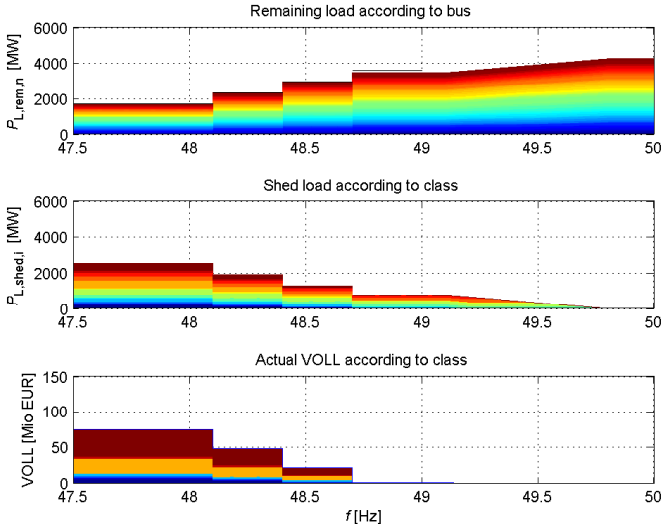

Fig. 14. Static analysis of the load shedding system – CL-UFLS with adapted C-UFLS

F. Numerical Results

In the remainder of this section, numerical simulation results according to the disturbance scenario defined above will be

presented. The system is simulated with a constant time step size of 10 ms. Event-handling as described in [35] is performed for important system events outside of the normal step size in order to capture the exact instants of significant discontinuous changes in the dynamics.

In all result plots (Figures 15, 17, 18, and 19), the structure is as follows: from top to bottom, the rotor angles, the generator frequencies, the measured bus frequencies (by PLL measurement), the remaining load at the buses and the totally incurred value of lost load are shown. The latter is based on the assumption that the outage duration is equal to 1 hour, which may be realistic in the case of a soft load shedding scheme which contains the disturbance and enables quick reactivation of the shed load. In the case of a more significant impact on the system (which is shown in Case 1), an outage time of 1 hour will probably be an under-estimation. As the duration of the outage depending on the disturbance and system reaction is not modeled in this work, this point has to be kept in mind when comparing the results.

Note that the rotor angles are simulated without a fixed reference. Thus, if the entire group of rotor angles "floats" through the angle space together, this does not cause any problems. Relevant is only the rotor angle *difference* between the generators.

1) No Islanding, C-UFLS: The first case, which includes only conventional load shedding and no controlled islanding, is shown in Fig. 15. After the disturbance at 0.1 s, the rotor angles split themselves into two groups. The first group corresponds to the generators 103 and 111, while the second group contains the rest of the generators. The angles of the first group, which is located in the direct vicinity of the fault, deviate significantly from the rest of the generator angles. This would cause these two generators to fall out of step and to consequently be tripped by the out-of-step relay after a certain number of asynchronous cycles, which is not explicitly modeled.

At the same time, the frequencies of generators 103 and 111 decay to values below 47.5 Hz, which would also cause them to trip. Note that this significant spread between the two deviating generators and the rest of the system happens although they stay connected to the rest. The reason for this is the long "electrical distance" between the vicinity of the fault and the rest of the grid. This is also reflected in the measured bus frequencies, which show large deviations at a group of buses and almost no deviation in the rest of the system. The deviating group corresponds to the frequencies of buses 103, 104, ..., 112, all of them located near the fault location.

The conventional load shedding system only reacts on the buses where under-frequency is detected. For that reason, the disturbance results only in slight load shedding during the simulation, which takes place on the buses with under-frequency mentioned above. However, if the tripping of generators by under-frequency and out-of-step relays was explicitly modeled here, a larger lack of active power would arise in the whole

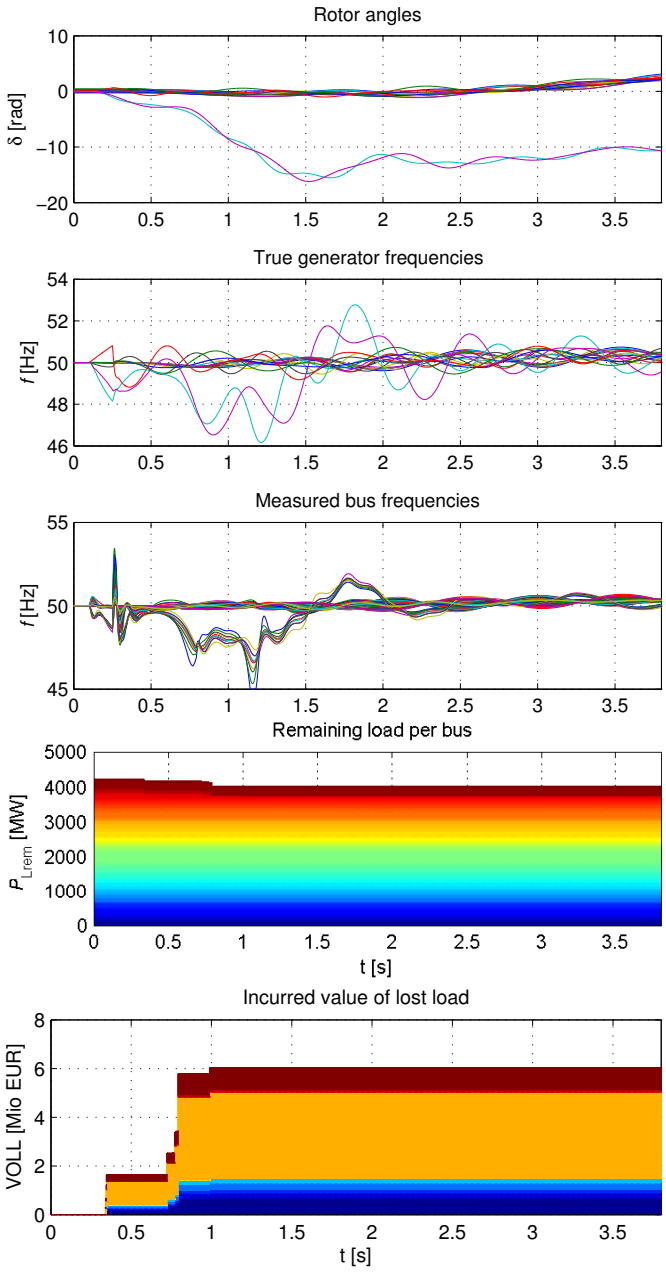

Fig. 15. Simulation result for case 1: no islanding, C-UFLS

system which would further provoke frequency decrease and it would likely lead to a widespread blackout. The value of lost load, which is incurred by the load shedding and shown in the lower plot, reaches 6 million Euros after 1 second. This result is based on the simulated situation (without generator tripping) and on the assumption that the supply is restored after 1 hour, which may be a significant under-estimation. The real VOLL in such a case would most probably much higher.

In order to prevent the spread of the failure throughout the whole system by cascading failures, an effective emergency control action would be the application of a controlled islanding strategy as shown in the next case.

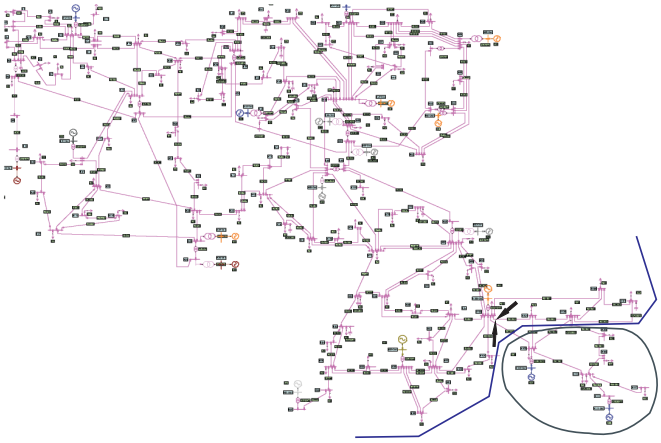

Fig. 16. Splitting of the power system after controlled islanding

2) Controlled Islanding, C-UFLS: The result of the second case is shown in Fig. 17. Time of occurrence of the fault and fault clearing time are the same as in Case 1. In Case 2 we study the effect of controlled islanding. After the detection of the fault, the rotor angle deviation and the active power generation and load are given as an input to the controlled islanding algorithm. After 0.245 s, the lines to be tripped are identified. These are the lines between buses 103-104, 103-105 and 105-108. The tripping of the lines is activated at $t = 0.75$ s. According to this strategy the system is partitioned into two islands. The load-generation active power imbalance, as calculated from the controlled islanding algorithm, is a deficit of 64 MW in the smaller southeast island and an excess of 199.4 MW generating power in the bigger island[3]. As a result, a load shedding of 64 MW might take place in the end, which is about 1.51 % of the total load. The amount of actual load to be shed may however vary due to the effect of transient dynamics and the primary controllers. The load shedding system in place is only the conventional one as before.

The controlled islanding strategy has two main effects: The two generators that exhibit the rotor angle deviation are now isolated in a small island in the south-east corner of the system (see Fig. 16), supplying only a number of loads at the buses in the vicinity. Because of this, their angle difference to the rest of the system becomes irrelevant, and only the angle difference to each other is of interest. Due to this fact, they would not be tripped by their out-of-step relays. A further effect of the islanding is that the load buses 104, 105, 106 and 107, which were before in the group of buses with decaying frequency because of the proximity to the deviating generators, are now associated with the bigger island (as this leads to a smaller load-generation imbalance in the two islands) and are therefore ”pulled” back towards the nominal system frequency of 50 Hz.

However, even if the system is now stabilized, there is a

[3]The transmission losses are not taken into account in the controlled islanding algorithm.

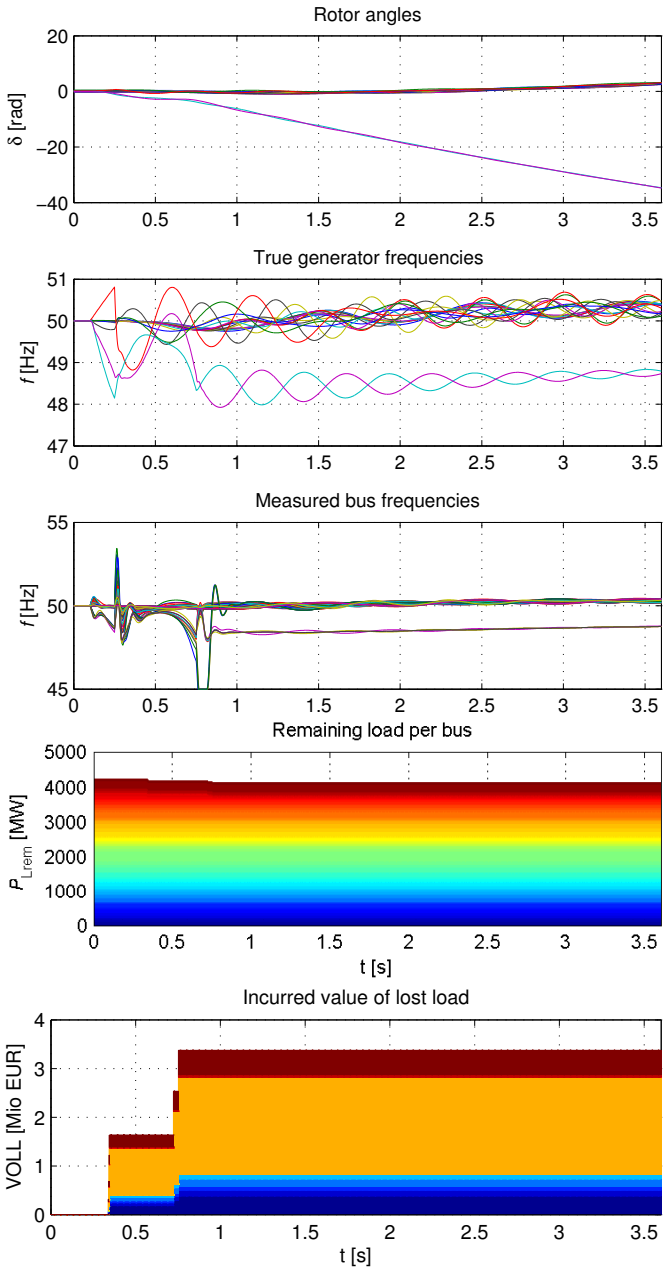

Fig. 17. Simulation result for case 2: controlled islanding, C-UFLS

deviation of more that 1 Hz in the steady-state frequency of the smaller island. In the following case the additional customer-level load shedding policy will be used so as to alleviate this effect.

Note that in the measured bus frequencies a transient can be seen, which is caused by a voltage spike due to the islanding. However, this does not affect the load shedding system, as the transients decay well below the detection time delays of the load shedding systems.

3) Controlled, Islanding, CL-UFLS and unchanged C-UFLS: The simulation of the third case is presented in Fig. 18. Now, the customer-level load shedding is activated, while the conventional load shedding system remains unchanged. The

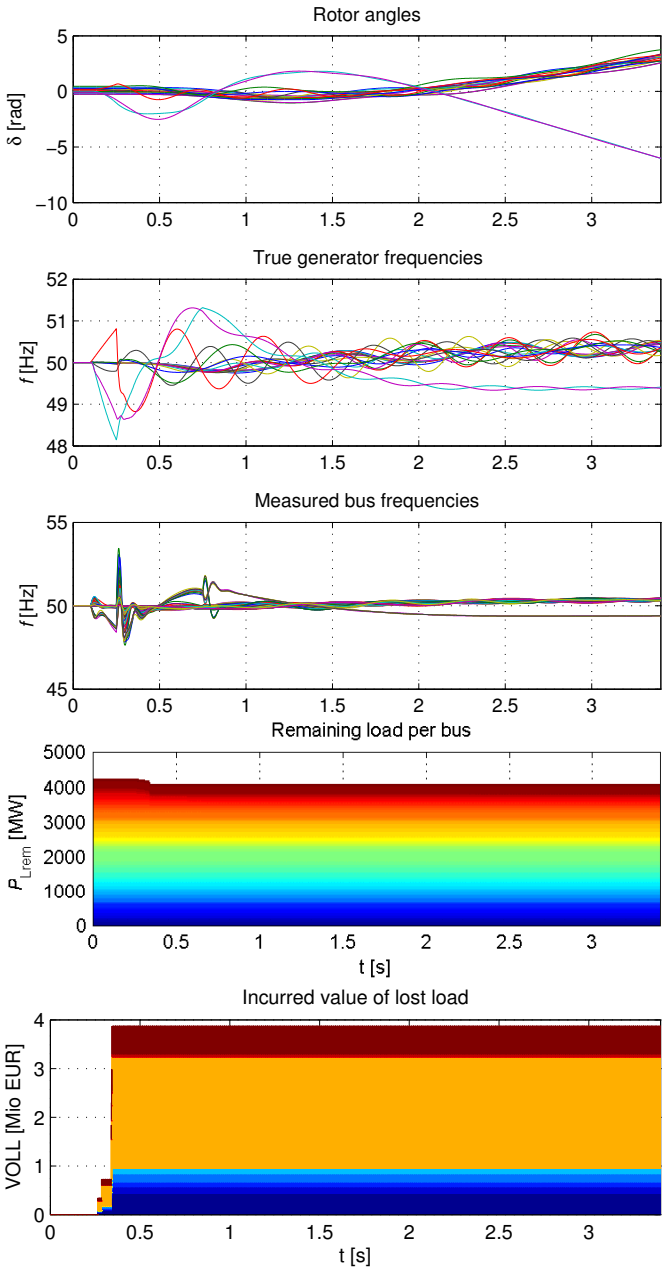

Fig. 18. Simulation result for case 3: controlled islanding, CL-UFLS and unchanged C-UFLS

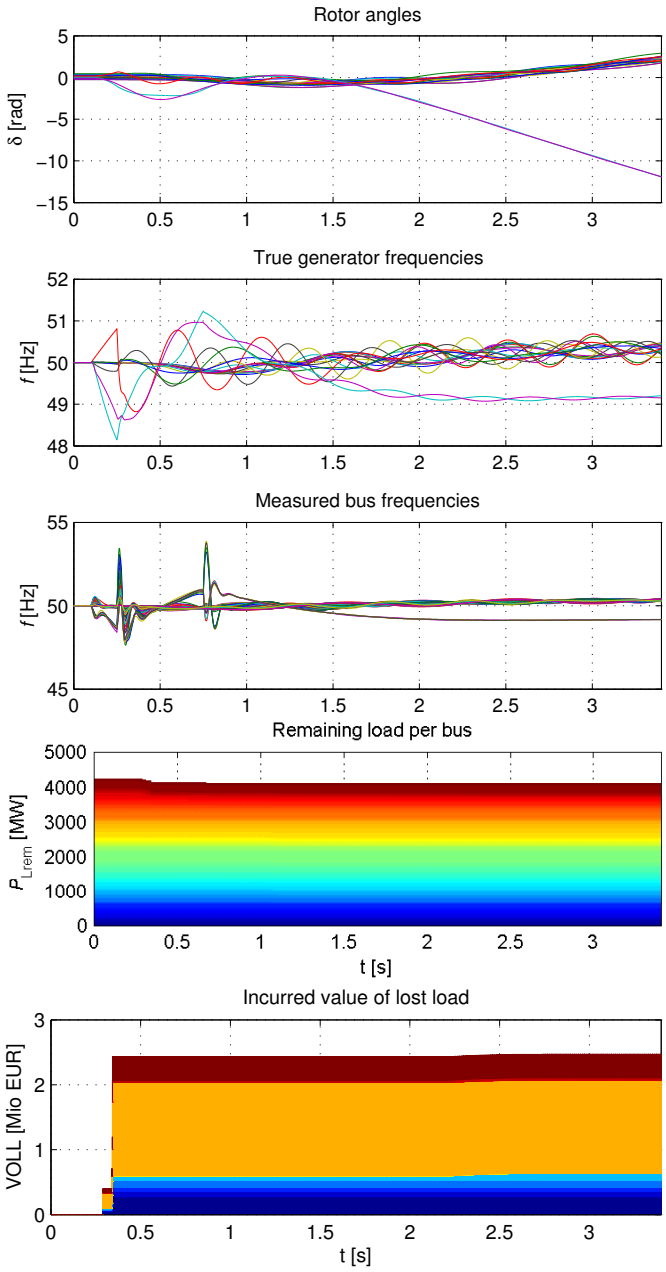

Fig. 19. Simulation result for case 4: controlled islanding, CL-UFLS and adapted C-UFLS

static analysis shown in Fig. 13 reflects that situation. The conventional load shedding starts at a frequency of 49 Hz, while the CL-UFLS is applied gradually from 49.8 Hz. The frequency response in Fig. 18 highlights the benefit of the applied technique since the frequency steady-state deviation is limited to around 600 mHz.

4) Controlled, Islanding, CL-UFLS and adapted C-UFLS: Finally, the results of simulating the fourth case are presented in Fig. 19. The difference to the previous simulation is the adaptation of the conventional load shedding system in the presence of customer-level load shedding, which is actually the difference between Fig. 13 and Fig. 14. In this case the frequency steady state deviation is around 800 mHz. The main advantage obtained from the adaptation of the conventional load shedding is that the value of lost load, shown in the lower plot, reaches only 2.5 million Euros while with the same assumptions in the previous case it was around 4 million Euros. This is due to the fact that conventional load shedding stages are triggered on a smaller number of distribution feeders than in the previous case.

V. Conclusion

This paper presented a combination of a k-means-based controlled islanding approach with a graceful customer-level under-frequency load shedding. It was shown that the two methods together, although in principle independent, exhibit significant synergies and provide an effective means for disturbance mitigation. Controlled islanding is a suitable means

to counteract angle instability by isolating the group of coherently oscillating generators, which can prevent the triggering of out-of-step relays. The fact that the calculations take place in real time helps to take into account the instantaneous power production, including, potentially, intermittent sources. The presented algorithm is therefore adaptive, and at the same time modular, as it can incorporate several different criteria for the system partitioning.

Customer-level load shedding should be seriously considered for practical implementation if the currently apparent convergence of energy and information technologies proves to provide a suitable platform for interconnecting a multitude of individual consumer appliances. In this case, fast and low-customer-impact load reduction can be achieved, while the distribution system is still able to serve vital loads and take infeeds from Distributed Generation units. This may be a determining factor for maintaining the security of supply in future power systems.

Opportunities for further work are e.g. the development of an organizational concept for coordinating a multitude of distribution systems with different customer-level load shedding penetrations, the investigation of the effects of Distributed Generation on the load shedding schemes, and the study of daily load profiles and corresponding time-varying frequency threshold assignment for the appliance classes.

Acknowledgements

The authors would like to thank the European Commission for funding the projects *IRENE-40*, FP7-ENERGY-2007-2-TREN and *VIKING*, FP7-ICT-SEC-2007-1. Special thanks go to Dr. Turhan Demiray for the provision of a flexible dynamic power system simulation environment in MATLAB® and for his kind support during the implementation of the model.

References

[1] H. Li, G.W. Rosenwald, J. Jung, and C. Liu. Strategic power infrastructure defense. *Proceedings of the IEEE*, 93(5):918 –933, May 2005.

[2] H. You, V. Vittal, and X. Wang. Slow coherency-based islanding. *Power Systems, IEEE Transactions on*, 19(1):483–491, Feb. 2004.

[3] J. H. Chow. *Time-Scale Modeling of Dynamic Networks with Applications to Power Systems*. New York: Springer–Verlag, 1982.

[4] Kai Sun, Da-Zhong Zheng, and Qiang Lu. A simulation study of OBDD-based proper splitting strategies for power systems under consideration of transient stability. *Power Systems, IEEE Transactions on*, 20(1):389 – 399, Feb. 2005.

[5] A. Peiravi and R. Ildarabadi. A fast algorithm for intentional islanding of power systems using the multilevel kernel k-means approach. *Journal of Applied Sciences*, 9(12):2247–2225, 2009.

[6] C.G. Wang, B.H. Zhang, J. Shu, P. Li, and Z.Q. Bo. A fast method for power system splitting boundary searching. In *Power Energy Society General Meeting, 2009. PES '09. IEEE*, 2009.

[7] S. Najafi. Evaluation of interconnected power systems controlled islanding. In *PowerTech, 2009 IEEE Bucharest*, Jun. 2009.

[8] D. Chaniotis and M.A. Pai. Model reduction in power systems using Krylov subspace methods. *Power Systems, IEEE Transactions on*, 20(2):888 – 894, May 2005.

[9] C. M. Bishop. *Pattern Recognition and Machine Learning*. New York: Springer–Verlag, 2006.

[10] Thomas H. Cormen, Charles E. Leiserson, Ronald L. Rivest, and Clifford Stein. *Introduction to Algorithms*. Cambridge, Massachussets: MIT Press, 2001.

[11] Power Systems Test Case Archive, College of Engineering, University of Washington. URL: http://www.ee.washington.edu/research/pstca/.

[12] Bonian Shi, Xiaorong Xie, and Yingduo Han. WAMS-based load shedding for systems suffering power deficit. In *Transmission and Distribution Conference and Exhibition: Asia and Pacific, 2005 IEEE/PES*, 2005.

[13] R.A. Hooshmand. Optimal design of load shedding and generation reallocation in power systems using fuzzy particle swarm optimization algorithm. *J. Applied Sci.*, 8:2788–2800., 2008.

[14] S. K. Sen, Anish Deb, A. Roy, and Asit K. Datta. A method for tracking power line frequency with millihertz resolution and high/low cut-off. *Electric Power Systems Research*, 23(3):239 – 243, 1992.

[15] M. Karimi-Ghartemani and M. R. Iravani. Wide-range, fast and robust estimation of power system frequency. *Electric Power Systems Research*, 65(2):109 – 117, 2003.

[16] ENTSO-E. Continental Europe (CE) Operation Handbook. URL: http://www.entsoe.eu, 2004.

[17] P.M. Anderson and M. Mirheydar. An adaptive method for setting underfrequency load shedding relays. *Power Systems, IEEE Transactions on*, 7(2):647 – 655, May 1992.

[18] J.G. Thompson and B. Fox. Adaptive load shedding for isolated power systems. *Generation, Transmission and Distribution, IEE Proceedings-*, 141(5):491 – 496, Sep. 1994.

[19] V.V. Terzija. Adaptive underfrequency load shedding based on the magnitude of the disturbance estimation. *Power Systems, IEEE Transactions on*, 21(3):1260 – 1266, Aug. 2006.

[20] R.V. Fernandes, S.A.B. de Almeida, F.P.M. Barbosa, and R. Pestana. Load Shedding – Coordination between the Portuguese transmission grid and the distribution grid with minimization of loss of distributed generation. In *PowerTech, 2009 IEEE Bucharest*, Jun. 2009.

[21] Steven R. Harper, Deborah L. Thurston, and Philip T. Krein. The effects of dynamic residential load participation : penetration levels for operational impact on reliability. *Int. J. Critical Infrastructures, Vol. 3, Nos. 1/2, 2007*, Vol. 3(1-2):221 – 234, 2007.

[22] D. Craciun, S. Ichim, and Y. Besanger. A new soft load shedding: Power system stability with contribution from consumers. In *PowerTech, 2009 IEEE Bucharest*, Jun. 2009.

[23] F.C. Schweppe, R.D. Tabors, J.L. Kirtley, H.R. Outhred, F.H. Pickel, and A.J. Cox. Homeostatic utility control. *IEEE Transactions on Power Apparatus and Systems*, PAS-99:1151–1163, 1980.

[24] J.A. Short, D.G. Infield, and L.L. Freris. Stabilization of grid frequency through dynamic demand control. *Power Systems, IEEE Transactions on*, 22:1284–1293, 2007.

[25] Junji Kondoh. Autonomous frequency regulation by controllable loads to increase acceptable wind power generation. *Wind Energy*, 2009.

[26] V. Ricquebourg, D. Menga, D. Durand, B. Marhic, L. Delahoche, and C. Loge. The smart home concept : our immediate future. In *E-Learning in Industrial Electronics, 2006 1ST IEEE International Conference on*, pages 23 –28, 18-20 2006.

[27] S. Koch, M. Zima, and G. Andersson. Potentials and applications of coordinated groups of thermal household appliances for power system control purposes. In *Proceedings of IEEE - PES/IAS Conference on Sustainable Alternative Energy. Valencia, Spain*, 2009.

[28] Patrick McDaniel and Stephen McLaughlin. Security and privacy challenges in the smart grid. *IEEE Security and Privacy*, 7(3):75–77, 2009.

[29] Peter Cramton and Jeffrey Lien. Value of lost load (available online). 2000.

[30] frontier economics and RWE AG. Cost of electricity supply interruptions (Kosten von Stromversorgungsunterbrechungen, available online in German). URL: http://www.frontier-economics.com/, Jul. 2008.

[31] Richard S.J. Tol. The value of lost load. *ESRI Working Paper No. 214*, 2007.

[32] Standard load models for power flow and dynamic performance simulation. *Power Systems, IEEE Transactions on*, 10(3):1302 –1313, Aug. 1995.

[33] P. M. Anderson and A. A. Fouad. *Power System Control and Stability*. IEEE Computer Society Press, 2002.

[34] NEPLAN Official Website. http://www.neplan.ch.

[35] Turhan H. Demiray. *Simulation of Power System Dynamics using Dynamic Phasor Models*. PhD thesis, Diss. ETH No. 17607, available online from ETH Zurich, Switzerland, 2008.

[36] Ifigeneia Stefanidou and Maria Zerva. Control strategies for underfrequency load shedding (Semester thesis, available online). ETH Zurich, EEH – Power Systems Laboratory, 2009.